GALECTIN-3 AND THE MODULATION OF ANTITUMOR IMMUNITY

by
Alexandra B. Pucsek

A dissertation submitted to Johns Hopkins University in conformity with the requirements for the degree of Doctor of Philosophy

Baltimore, Maryland
March 2020

ABSTRACT

In the last decade, galectin-3 has emerged as an important player in the development and progression of cancer, favoring immune suppression and dysfunction at disease sites. While this protein is a known tumor-promoting factor, its unique properties make the mechanisms of its functions difficult to study, and impede the development of therapies against it. Galectin-3 recognizes and binds β-galactoside carbohydrate residues through a highly-conserved C-terminal domain (CRD). It uniquely self-associates into homo-oligomers through a disordered N-terminal domain (NTD). We have previously shown that immune responses against galectin-3 are protective in pancreatic ductal adenocarcinoma (PDAC), and that its knockout in a mouse model of tumor tolerance improves effector function of antitumor $CD8^+$ T cells and increases duration of tumor-free survival, suggesting a suppressive role for galectin-3 in antitumor immunity. The mechanisms of this suppression remain unknown.

To learn whether galectin-3 could be a target for preventative therapeutics, I examined disease progression in a genetically engineered mouse model of PDAC development upon abrogation of galectin-3. I saw no significant change in lesion development or overall survival, indicating that galectin-3 is unlikely to be a good target for prevention strategies. In an effort to further study its mechanisms of immune suppression, I developed an assay to model galectin-3-mediated $CD8^+$ T cell suppression, and showed that this assay allows successful activation of antigen-specific $CD8^+$ T cells *in vivo* and detection of effector cytokines after re-stimulation *in vitro*. Through this assay we expect to learn how the discrete galectin-3 binding

domains each impact its suppressive functions. Finally, I examined a transgenic mouse strain with a deficiency in dendritic cell populations, which regains those populations upon abrogation of galectin-3. This puzzling phenomenon remains unsolved, but I posit some lines of future inquiry that could elucidate this phenomenon, and inform our studies of galectin-3-mediated T cell modulation as well.

Galectin-3 has been known as a factor in tumor permissiveness for decades, but has not yet been effectively targeted. Determining the mechanisms behind galectin-3-mediated immune cell modulation in the context of tumor will allow it to be targeted effectively, and could lead to better immunotherapeutic outcomes.

Advisor

Dr. Elizabeth M. Jaffee, MD (Reader)

Thesis Committee

Dr. Ronald L. Schnaar, PhD

Dr. Douglas N. Robinson, PhD (Reader)

Dr. Joel L. Pomerantz, PhD

Dr. Andrea L. Cox, MD, PhD

ACKNOWLEDGMENTS

I would like to thank Dr. Jaffee, my thesis advisor, for the time and effort she has put into fostering me as a researcher. She has allowed me to learn to be independent in all aspects of my work, and given me time and space to navigate both my developing career and my home life. Liz, I so appreciate your belief in me and the example that you give us every day. I feel proud to be a part of what you've built in this research group. I also must give great thanks to Dr. Todd Armstrong, who has never turned me away or been "too busy", whether I'm storming his office with a dire research emergency or a horrible pun. Thank you for lending an ear, time after time, and for putting out the fires when nobody else knows how. Great thanks also to my lab mates, who have witnessed the madness firsthand. To the former, current, and future members of the Jaffee Lab (& co.), thank you all for lending an ear, for putting up with my grouchiness one moment and my elation the next. We have a funny little family here and I'm glad to have worked with all of you. Special thanks to James. I have yet to find a lab problem you can't solve—same day!—and I hope I never do.

I must extend special thanks to my thesis committee members, Drs. Ronald Schnaar, Douglas Robinson, Joel Pomerantz, and Andrea Cox. Ron, your glycobiology expertise was essential to my grasp of this project. Thank you for your patience as I navigated an arm of biochemistry that was entirely foreign to me. Doug, your expertise in protein purification was a lifeline for me when this project threatened to slip out of my grasp. Thank you, and all of your lab members, for letting me make a second home in Physiology and for treating me like one of the group from the start. Joel, thank you for your continuing advice on my molecular biological approaches,

and for everything you've done for the Graduate Program in Immunology as director. We are privileged to have you. Andrea, thank you for helping me keep my experiments rigorous and for always having a perspective I hadn't considered. Your input and ideas have been instrumental.

I'd like to thank my extended Hopkins family, especially the Powell Lab and the Robinson Lab, for all of their support and friendship. You're an amazing group of researchers and I'm privileged to call you my peers. Thanks also to Drs. Christopher Gamper and Brian Ladle, who gave me a chance here as a technician, and have continued to offer friendship and mentorship. I truly wouldn't be here at Hopkins without you. Thanks for opening the door for this life-changing opportunity. One huge thank you to the entire Johns Hopkins community. We're navigating a worldwide disaster right now, and I'm watching you come together in unprecedented ways. Thank you for being an inspiration and an example.

Finally, I would like to thank my friends and family. To my friends who have kept in touch across great distance and great peril, thank you for reaching out, even when I was in no state to reach back reciprocally. My mental health is indebted to you. To my extended family, who may not understand why in the world I'm still "in school", thanks for loving your eccentric niece/granddaughter/cousin anyway. I should be able to stay in touch a little better now. I have to extend special thanks to my cousin Tommy. Thank you for that one crazy wee-hours Facebook chat where you helped me get my foot in the door for a technician interview at Hopkins. I had no idea how much that chat would change my life. Let's hope we're making Autumn proud. To my parents, two intellectual giants (whether or not they know it), I owe you both so much. You have

made me your priority for my entire life, and I've had the privilege of unfettered opportunity as a result. Thank you for believing in me even when I was failing, and thank you for raising me to push myself and strive for more. This is your achievement as much as it is mine. Last, but most importantly, I want to thank my best friend and partner, my husband Blake. I would never, never, never have gotten through the lows of this experience without your unflagging faith in me and your commitment to living as a true partner. Thank you for being an amazing father to the most amazing kid on the planet, for helping me be a mom and a nascent scientist, and thank you above all for loving me when I feel entirely unlovable. You make my life worth living, and this work is dedicated to you.

TABLE OF CONTENTS

LIST OF FIGURES

CHAPTER 1: Introduction

Galectin-3: A Multifunctional Modulator of Inflammation, Motility, and Immunity

In recent years, cancer immunotherapy has dramatically altered the landscape of cancer treatment, both in accompaniment with and as an alternative to conventional chemoradiotherapy (1). Immunotherapy, however, remains an imperfect solution due to our incomplete understanding of the factors that work alongside cancerous cells to suppress and silence the antitumor functions of the immune system, and evasion of antitumor immunity is now considered a hallmark of cancer (2). It is therefore important not only to research new immunotherapeutic approaches, but also to further our understanding of the factors that can contribute to the failure of these treatments in certain patient populations. Extensive study has shown the protein galectin-3 to be capable of promoting tumor growth, invasion, and metastasis, while also contributing to adaptive immune suppression in a tumor context (3,4).

Galectin-3 is a 31kD β-galactoside-binding protein, unique in structure among galectin family members for its N-terminal disordered tail domain (NTD), and C-terminal carbohydrate recognition domain (CRD) typical of mammalian galectins (5,6). It is ubiquitously produced and can exert functions both intracellularly and extracellularly (7), but is most studied in disease contexts, where it generally takes part in dysfunctional regulation. In the cytosol, galectin-3 is known as a binding partner of apoptotic regulators such as B-cell lymphoma 2 (BCL2), CD95 (APO-1/Fas), and Nucling (8–10), and also regulates cell proliferation, differentiation, and survival through interactions with Ras proteins and Akt (11,12). At the cell surface, galectin-3

canonically binds N-acetyllactosamine repeats in the branched N- and O-linked oligosaccharides of the glycocalyx (13,14). These binding events are understood to occur through the CRD, while the NTD has been understood to allow oligomerization of galectin-3 molecules (3,15). More recently, it has been shown that intermolecular interactions between galectin-3 proteins may also occur through CRD-CRD or NTD-CRD interactions (16). These oligomerization events lead to the formation of multivalent assemblies of galectin-3 and lattice formation upon binding of its extracellular glycan ligands. Such lattices may influence the signaling downstream of affected surface proteins which carry the target glycan residues by causing clustering that can impede or enhance signal transduction into the cell (17). Multivalent galectin-3 oligomers also influence the ability of cells to interact with the extracellular matrix (ECM) and migrate to distal sites (4,18,19). These diverse functions are often found to be immune modulatory, as galectin-3 is known to play roles specifically in the contexts of tumor, autoimmune disease, and tissue damage and repair (7).

Antitumor Immune Functions of $CD8^+$ T cells and Antigen-Presenting Dendritic Cells

The last fifteen years have brought a new appreciation of how crucial immune cell function is for the control and rejection of tumors. Our new understanding of how immune cell functions are subverted by tumor cells for eventual immune evasion and escape has given rise to immunotherapy, a set of treatments that aim to restore immune cell effector functions while removing the brakes from immune regulation (1). Two cell types which play key roles in tumor control are cytotoxic $CD8^+$ T cells and

dendritic cells (DCs), and both have arisen in our research as cell types which may interplay with galectin-3 in the tumor microenvironment (20).

$CD8^+$ T cells are potent killers of tumor cells, but can also be silenced upon entry into the tumor microenvironment (21). They respond best to tumors with a high mutational burden, which are more likely to produce antigens these T cells can recognize (22,23). Naïve $CD8^+$ T cells become activated upon meeting their cognate antigen presented on antigen-presenting cells (APCs) bearing the class I major histocompatibility complex (MHC class I) in the lymph node, undergo activation, and can then traffic to the tumor site and perform killing functions against cells bearing tumor antigens through the release of inflammatory cytokines and cytotoxic granules (24).

The surface receptors that normally function to dampen the cytotoxicity of $CD8^+$ T cells by preventing damage associated with an overactive immune response can also be co-opted by tumors to evade killing. The best-studied surface receptor that mediates such interactions is PD-1 (CD279), which is now known as a checkpoint molecule due to its well-documented $CD8^+$ T cell inhibition. PD-1 on the T cell binds to a ligand, usually PD-L1 (B7-H1, CD274) or PD-L2 (B7-DC, CD273) (25). In the context of cancer, tumor cells can express these ligands, transducing inhibitory signals into the cytotoxic T cell and preventing further instances of killing. PD-1 is now the target of immune checkpoint antibody blockade strategies, which are promising components of immunotherapy. However, despite these new therapies, other factors beyond canonical checkpoint molecules continue to interfere with $CD8^+$ T cell effector function in the context of tumor.

Dendritic cells (DCs) are professional antigen-presenting cells (APCs), and drive adaptive immune responses by priming naïve $CD4^+$ and $CD8^+$ T cells (26). There are many distinct DC subsets, but most are primarily identified by expression of the surface marker CD11c (27). In their role as presenters of antigen both in secondary lymphoid organs and at the tumor site, they have arisen as a critically important arm of the antitumor immune response (28). Their cross-presentation of tumor associated antigens on MHC class I is a cornerstone of the $CD8^+$ T cell antitumor response, and is necessary both to prime naïve $CD8^+$ T cells and to drive their cytotoxic function at the tumor site (29). Defects in antigen cross-presentation are common dysfunctions of DCs in the tumor context (30–32), and these remain some of the less-studied components that can disrupt current immunotherapeutic approaches. Galectin-3 has been implicated in processes that target both of these crucial cell types, forming the impetus behind my studies of this protein.

Galectin-3 in Immune Suppression and Tumor Promotion

Galectin-3 is one of the major factors that leads to the dysfunction of antitumor immune cells (3). Its functions result in a tumor-promoting microenvironment through the effects it has on the tumor cells themselves, on the stromal cells of the microenvironment, and on antitumor immune effector cells.

The internal and external functions facilitated by galectin-3 on tumor cells are directly involved in multiple hallmarks of cancer. It contributes to the transformation of tumor cells through interactions with oncogenic Ras proteins, specifically KRAS (33). In the cytosol, it can suppress apoptotic signals, due in part to its homology with the

protein BCL2, which allows it to traffic to the mitochondria to block apoptosis (34,35). Importantly, galectin-3 increases the metastatic potential of tumor cells and promotes invasion, metastasis, and colonization of distal sites by mediating cell-cell adhesion between tumor cells (4), promoting the epithelial-to-mesenchymal transition (18), and facilitating tumor cell interactions with the extracellular matrix (19). It also promotes angiogenesis at the tumor site, an important factor for tumor cell survival in hypoxic conditions (36).

The effects of galectin-3 on $CD8^+$ T cell antitumor functions come from multiple angles at once. Galectin-3 can decrease the affinity of the T-cell receptor (TCR) for MHC class I-antigen complexes by forming galectin-3-TCR lattices, sequestering TCRs from their co-receptor CD8 (37). Other studies have shown that galectin-3 can induce $CD8^+$ T cell apoptosis through interactions with CD29 and CD7 (38). Our lab has shown that galectin-3 binds the suppressive signaling molecule LAG-3, and proposed that such binding could cluster surface LAG-3 and induce suppressive signals that dampen $CD8^+$ T cell antitumor effector functions at the tumor site (20).

Overview of Thesis Work

The overall goal of this thesis is to use a mouse model of cancer development to learn more about whether galectin-3 would be a viable target for preventative therapies, and to develop methods that allow us to determine the mechanisms by which galectin-3 suppresses antitumor $CD8^+$ T cells. This has been accomplished by:

1. Comparing pancreatic lesion development and overall survival in a genetically-engineered mouse model of pancreatic ductal adenocarcinoma

(PDAC) to age- and sex-matched mice with a genetic ablation of galectin-3, showing that removal of galectin-3 does not significantly impact temporal progression through the stages of PDAC development or survival at any time point.

2. Attempting the development of a new *in vitro* assay for the identification of putative galectin-3 binding partners on the $CD8^+$ T cell surface.
3. Developing an *in vitro* assay to assess the ability of galectin-3 to suppress *in vivo*-activated $CD8^+$ T cells upon re-stimulation, and using mutant galectin-3 proteins with loss of function of one or more galectin-3 binding domain to determine how these domains each impact suppressive potential.
4. Exploring the link between galectin-3 and dendritic cell subsets in a tumor-tolerant mouse model to propose new avenues of inquiry into its immune modulatory capabilities.

CHAPTER 2: Effect of Galectin-3 Abrogation in a Mouse Model of Pancreatic Ductal Adenocarcinoma (PDAC) Development

Rationale and Experimental Design

Pancreatic ductal adenocarcinoma (PDAC) is currently one of the deadliest cancers, and one of the least likely to be detected before metastases develop and worsen disease outcomes (39). Additionally, PDAC is often poorly infiltrated by antitumor immune cells, which can make immunotherapies a less effective treatment strategy (40). Our lab works extensively on determining how the components of the PDAC tumor microenvironment contribute to tumor-permissiveness, and how these components can be perturbed to make inroads for immunotherapy and influence better treatment outcomes for patients. In a previous study of PDAC patients receiving two whole-cell GM-CSF-secreting pancreatic tumor cell lines as vaccine, our lab showed that an elevated level of serum anti-galectin-3 IgG was found to be correlated with improved disease outcome (disease-free survival >3 yrs) (20). 67% of patients who survived longer than three years post-treatment showed twofold or higher increase of anti-galectin-3 antibody titers, while only 9.5% of patients who survived less than three years showed a similar increase. Additionally, sera taken from these good-responder patients were capable of inhibiting galectin-3-mediated suppression of healthy donor $CD8^+$ T cells *in vitro* (20). Galectin-3 has already been described as a promoter of a tumor-permissive immune microenvironment as detailed in Chapter 1, and the data from our lab indicate that it may play such a role in PDAC specifically.

To begin such study, we wanted to discover the effect of galectin-3 abrogation

on pancreatic lesion development and overall survival in a mouse model of PDAC development and progression. The mouse strain *LSL-KrasG12D/+;LSL-Trp53R172H/+;Pdx-1-Cre* (KPC) has been shown through histological and survival assessment to model the development and progression of human PDAC in a temporal manner (41). These mice carry an activated oncogenic Kras mutation as well as a dominant negative allele of the p53 tumor suppressor, both under the control of Pdx-1-Cre, driving expression specifically in pancreatic tissues (42). Mice develop low-grade pancreatic intraepithelial neoplasms (PanINs) between 4-6 weeks of age, with high-grade PanINs detectable at 8-10 weeks. By about 12 weeks of age, most KPC mice have begun to progress from PanINs to PDAC. Our lab has utilized the KPC mouse model to study the efficacy of tumor vaccines and immune modulators in preventing or slowing the development of PanINs and PDAC (43). To discover the effect of galectin-3 abrogation on this model, we crossed the parental strains of the KPC mouse model to matched-background *Lgals3*$^{-/-}$ (*galectin-3* KO) mice, then performed assessments of disease progression, immune cell infiltrate, and survival in age-matched cohorts of KPC and *LSL-KrasG12D/+;LSL-Trp53R172H/+;Pdx-1-Cre;Lgals3*$^{-/-}$ (KPC-G) mice.

Materials and Methods

Generation of LSL-KrasG12D/+;LSL-Trp53R172H/+;Pdx-1-Cre;Lgals3-/- *(KPC-G) Mice*

LSL-KrasG12D/+;LSL-Trp53R172H/+; and *Pdx-1-Cre* strains on a mixed 129/SvJae/C57Bl/6 background were a gift from Dr David Tuveson (Cold Spring Harbor Laboratory, Cold Spring, NY). These mice were backcrossed to the C57Bl/6 background for twelve generations as previously described (43). The two parental strains (*LSL-KrasG12D/+;LSL-Trp53R172H/+* and *Pdx-1-Cre*) are interbred to obtain KPC mice (42). Each of these strains was therefore crossed with *Lgals3*$^{-/-}$ (*galectin-3* KO) mice of a C57Bl/6 background to achieve *galectin*-3 homozygous KO animals of each parental strain. Genotypes were assessed by taking tail biopsies at 3 weeks of age and sending to Transnetyx for analysis with previously-developed genotyping protocols and primers. To generate the *Pdx-1-Cre, Lgals3*$^{-/-}$ mice, zygosity testing for Cre was necessary. A protocol for testing was generated under the advice of Charles River Laboratories, who processed the samples for zygosity testing. Animals homozygous for both *Pdx-1-Cre* and knockout of *galectin-3* were utilized as breeders for this parental strain. Upon interbreeding, roughly 25% of progeny were genotyped as *LSL-KrasG12D/+;LSL-Trp53R172H/+;Pdx-1-Cre;Lgals3*$^{-/-}$ (KPC-G). Animals were housed in the Johns Hopkins Animal Facility and cared for according to protocols approved by the Johns Hopkins Animal Care and Use Committee.

Histological Assessment of PanIN Lesions of Age-Matched KPC and KPC-G Mice

KPC and KPC-G mice were obtained by interbreeding as described previously, and genotypes were determined by analysis of tissue samples taken at three weeks of age and sent for remote genotyping by Transnetyx. As genotypes were determined, KPC and KPC-G progeny were randomized into cohorts on a rolling basis. In total, ten male and ten female mice of each genotype (KPC or KPC-G) were enrolled into each age group cohort (4 weeks, 6 weeks, 8 weeks, 10 weeks, 12 weeks, or 14 weeks). Upon reaching the desired age plus or minus two days, mice were sacrificed and pancreata harvested. Whole pancreata were fixed by 48 hour incubation in 10% formalin, then paraffin-embedded. Two sections were cut from each pancreas, with sections sampled 1 mm apart and mounted on the same slide in the same orientation. Slides were H&E stained. Histological assessment and PanIN grading was performed in conference with clinical pathologists, whereby both sections were examined for the presence of PanIN lesions, and/or PDAC. Samples were given scores of No PanIN, PanIN 1, PanIN 2, PanIN 3, or PDAC based on published protocols (41,44), and the presence or absence of concurrent pancreatitis in each sample was noted. The final PanIN grade for each mouse was determined by the highest-grade lesion present across two pancreatic sections from the same individual. PanIN scores were grouped into No PanIN, Low-Grade (PanIN 1 or 2), and High-Grade (PanIN 3 or PDAC), and results were graphed using GraphPad Prism software.

Immunohistochemical Assessment of KPC and KPC-G Mouse Pancreata

New slides were cut from FFPE pancreata of the KPC and KPC-G mice previously sectioned for H&E staining and PanIN grading. These slides were stained by immunohistochemical protocols developed by Johns Hopkins Oncology Tissue Services for the markers CD3 and CD11b to broadly characterize lymphoid and myeloid cell infiltrates in and around pancreatic lesions. Assessment of immune cell infiltrate was performed by examining slides under 10X and 100X magnification and recording qualitative comparisons of cell infiltrates while blinded to the genotype and age group of each sample, then un-blinding after assessment of all samples and comparing descriptions within groups for similarities and differences.

Survival Comparison of KPC and KPC-G Mice

As litters from interbred mice were genotyped, mice identified as KPC or KPC-G were placed into groups and their survival followed. In total, fifteen male mice and fifteen female mice of each genotype (KPC or KPC-G) were followed, for a total of thirty mice per genotype. Endpoint of the experiment was defined as either spontaneous death, or morbidity requiring sacrifice per animal protocols and conferences with veterinary staff. Survival data were graphed and median survival was compared between groups using GraphPad Prism software.

Results

Breeding and Housing of KPC-G Mice and Sensitivity to H. pylori

Initial attempts to breed KPC-G mice resulted in few to no progeny, and those that were born had severe health problems. Infection with *Helicobacter pylori* (*H. pylori*) of facility-housed mice is a common problem, and while our KPC mice had been regularly tested for this and found negative, the researcher who crossed the KPC parental strains (*LSL-KrasG12D/+;LSL-Trp53R172H/+* and *Pdx-1-Cre*) to *galectin-3* knockout animals had incurred a contamination during the breeding process. After discovering the contamination, we began the process of cross-fostering these parental strains to remove the infection. During this process, I found by literature review that galectin-3 plays a role in innate immunity against *H. pylori*, preventing its deep infiltration into gut tissue, and causing aggregation that contributes to bacterial killing and disease control (45). The cited study showed that *galectin-3* knockout animals infected with *H. pylori* were susceptible to significant weight loss and gut inflammation compared to wildtype animals, which was congruent with the phenotype of the few early KPC-G progeny we observed. Indeed, once the parental strains of the KPC-G mice were successfully cross-fostered, they bred robustly and birthed expected proportions of KPC-G progeny. It is important, therefore, that all future researchers planning to utilize any *galectin-3* knockout animals ascertain that they are kept free of this pathogen, particularly when utilizing *galectin-3* knockout in heavily genetically engineered strains such as KPC.

KPC-G Mice Have Delayed Onset of PanIN Lesion Development

KPC and KPC-G mice were enrolled into study groups by age on a rolling basis. Age groups enrolled were 4, 6, 8, 10, 12, and 14 weeks of age. At target age plus or minus two days, mice were sacrificed and whole pancreata fixed and sectioned for H&E staining. In conference with clinical pathologists, we scored pancreata by determining the highest-grade lesion present in each sample. After determining PanIN score for each sample, scores were separated into one of three possible groupings: No Disease (No PanIN), Low-Grade Disease (scores of PanIN 1 or PanIN 2), and High-Grade Disease (PanIN 3 or PDAC).

Both KPC and KPC-G mice are susceptible to the development of PanIN lesions, pancreatitis, and PDAC. However, mice in the KPC-G cohorts were more likely than their KPC counterparts to remain disease-free for a longer period of time. While both groups of 4-week-old mice included individuals at each of the three stages of disease progression, certain KPC-G mice remained disease-free longer than their KPC counterparts. While 6 weeks of age was the latest KPC time point with disease free individuals, disease-free KPC-G mice were sampled at both 8 weeks and 10 weeks of age (**Figure 1**). By 12 and 14 weeks of age, however, the KPC and KPC-G mice had equal proportions of mice in each disease group, and no individuals remaining disease free. Therefore, though PDAC development may have a later onset in some of these mice, disease progression is not slowed overall.

Immune Cell Infiltrate is Dependent on Disease State

FFPE pancreata from the PanIN scoring groups were then grouped by disease score and inflammation state, and two individuals from each group were chosen for a pilot immunohistochemical analysis. Serial sections were cut from each pancreas and stained in parallel for CD3 and CD11b, to mark lymphoid and myeloid cell infiltrates, respectively. These slides were blinded, then qualitatively analyzed to gauge differences in infiltrate between disease scores, inflammation state, and genetics, once again comparing KPC to KPC-G animals. Broadly and expectedly, larger myeloid infiltrates were seen within known PDAC lesions, while larger lymphoid infiltrates were seen in the presence of pancreatitis. These patterns were consistent across KPC and KPC-G, and the sample size of each genotype at each stage of disease was too small to discern a difference upon galectin-3 abrogation.

Figure 1: Galectin-3 abrogation does not significantly affect the timeline of PanIN lesion or PDAC development in the KPC mouse model. For each genotype, ten male and ten female mice were grouped to be followed at each age endpoint, then sacrificed for pancreas dissection. Pancreata were formalin fixed and paraffin embedded, then sectioned for H&E staining. Slides were scored based on highest disease grade observed across two sections per mouse. While no significant differences were observed in the timeline of lesion development or progress to PDAC, it is notable that KPC-G mice with no detectable disease persisted at 8 and 10 weeks of age, while no KPC mice past 6 weeks were disease-free.

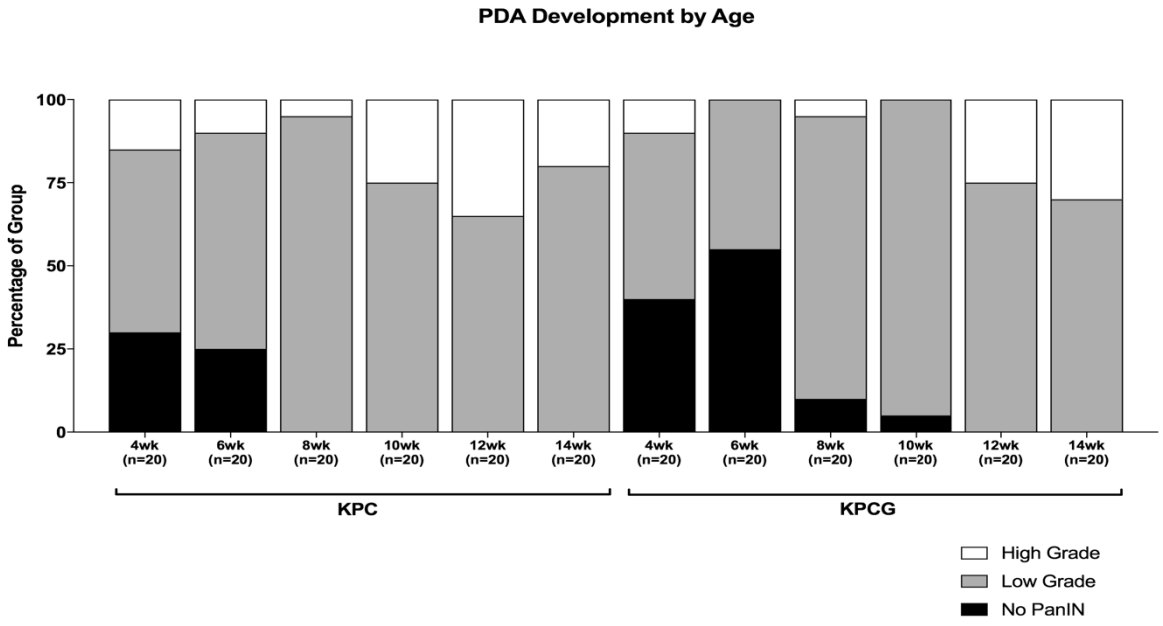

KPC and KPC-G Mice Have Sex-Specific Survival Benefits

To assess survival differences between KPC and KPC-G mice, animals were genotyped at three weeks of age, enrolled into either the KPC or KPC-G group respectively, and followed to an endpoint of either spontaneous death or morbidity requiring euthanasia per research animal protocols. Thirty mice were followed in each group, with male and female mice equally represented. At the conclusion of the survival experiment we observed interesting phenomena. While all KPC mice (n = 30) were deceased before 200 days, twenty percent (n = 6) of KPC-G mice were still living (**Figure 2A**). This difference becomes more stark when mice are analyzed by sex. All KPC-G mice that survived to 200 days or beyond were female, and the longest-lived survived for 294 days, 100 days longer than the longest-lived KPC mouse (**Figure 2B**). Additionally, when median survival of males and females in each group was assessed, a survival benefit was seen in KPC female mice as well. This is largely attributable to the fact that the KPC female cohort, as a whole, lasted the longest before its first individual reached an endpoint.

Figure 2: Survival of KPC and KPC-G mice is not significantly impacted by galectin-3 abrogation, but is sex-specific. A. The survival comparison between KPC and KPC-G mice shows no difference in median survival, but does indicate a subset of KPC-G mice that persist longer than other individuals. **B.** When survival is analyzed by sex, it can be seen that all longer-lived KPC-G mice are female. Additionally, female KPC mice seem to have a survival benefit apparent in longer cohort survival before the first death. While survival differences do not appear to be based on loss of galectin-3, the sex-based survival differences observed here should be taken into account by future researchers using this mouse model.

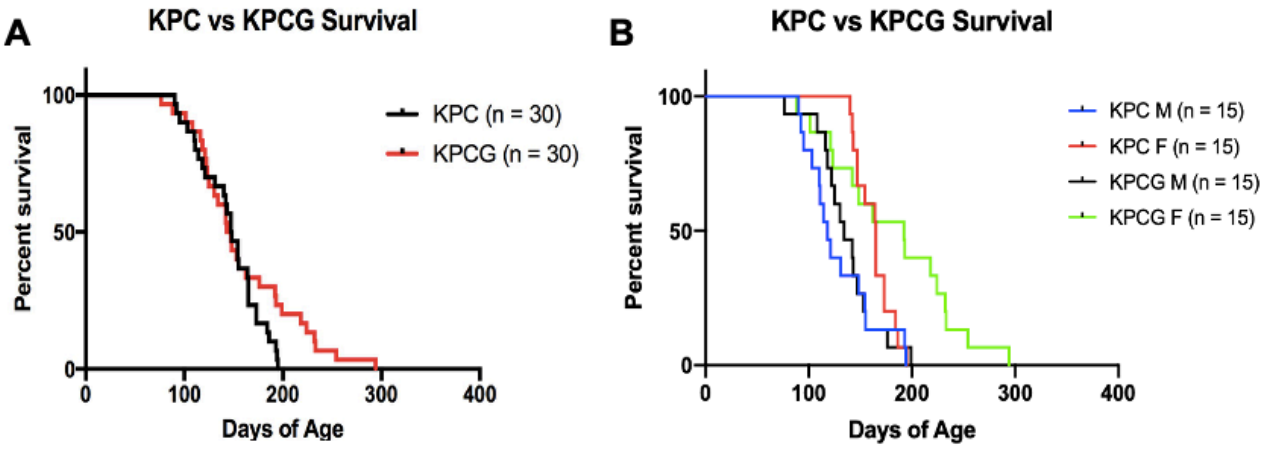

Discussion

Whether assessing PanIN development or immune cell infiltrate, no statistically significant differences were seen in KPC-G mice compared to KPC at baseline. There are, however, some differences that may warrant future study, and some pitfalls that should be avoided. First, the fact that there were disease-free KPC-G mice sampled at 8 and 10 weeks of age is of potential interest. The oldest disease-free KPC mice sampled were 6 weeks of age. This could indicate that a subset of KPC-G mice would be more sensitive to early treatment protocols. Our lab has previously shown that a Listeria monocytogenes vaccine against oncogenic Kras(G12D), along with Treg depletion, slows disease progression of KPC mice with low-grade, but not high-grade PanINs (43). If KPC-G mice are disposed to remain PanIN and PDAC-free for a longer period of time, they may be more likely to respond to such a vaccine protocol. Vaccine studies may also help to elucidate the immune mechanism by which galectin-3 suppresses antitumor responses. Translating the benefits observed in galectin-3 abrogation clinically is more challenging, as it is a ubiquitous protein with systemic effects, but confirming its immune mechanisms of action could elucidate further targetable pathways.

One major pitfall of my studies of PanIN lesion development and immune cell infiltrate is sampling error. In my study of immune cell infiltrate, for instance, too few samples were stained from each disease stage and inflammation state to be certain that differences in $CD3^+$ or $CD11b^+$ cell numbers were actually due to genotype rather than disease progression or the presence of pancreatic inflammation. The only notable phenomena seen in this study was $CD11b^+$ cells collecting in and near PDAC

tumors, and elevated $CD3^+$ cells in the presence of pancreatitis (data not shown), both of which are predictable and well-described in previous studies. Since disease outcomes in human PDAC depend on a confluence of these factors, future immunohistochemical comparisons of KPC and KPC-G mice should involve samples carefully paired based both on PanIN lesion stage and the degree of inflammation present, with multiple individual samples per group.

Additionally, and most critically, when sampling mice to compare PanIN lesions, I made the mistake of randomly assigning mice to groups after genotyping, and continuing enrollment in each group until the target number of samples was met, as defined by live mice sacrificed at the target age. The problem with this approach is that it introduces selection bias- for instance, if a mouse is enrolled in the 12 week age group, but dies by 8 weeks, the animal should still be considered part of the 12 week group, but noted to have met the endpoint before reaching the target age. In nearly every case, such animals will be found by necropsy to have high-grade lesions, PDAC, and/or severe pancreatitis. Disregarding the enrolled animals that met the endpoint before reaching the target age means that the later age groups were biased toward slower-progressing individuals. This casts doubt on any results from this portion of the study. A repeat sampling of mice would be necessary to confirm the present study's results. It may also be preferable to follow live mice with imaging technology such as ultrasound, in parallel with histological analyses, as this would give a more complete picture of when and how disease arises in KPC and KPC-G mice, and whether the two strains differ.

Following KPC and KPC-G mice for survival showed the interesting result that a subset of KPC-G females survived much longer than any other mice in this study. While KPC and KPC-G males had nearly identical survival curves, the longest-lived KPC-G female lasted 100 days longer than her KPC counterpart. Forty percent of KPC-G females outlived all other mice on the study, including the entire KPC female cohort. Future study could include periodic live imaging of mice during such a survival experiment to determine how disease was developing over time, in addition to immediate necropsy upon death to ascertain cause of death and its relation to disease state.

CHAPTER 3: Investigating the Relationship of Galectin-3 Binding Properties to its Suppression of Antitumor CD8$^+$ T Cells

Background and Rationale

Studies have repeatedly shown the ability of galectin-3 to suppress immune cell function and contribute to a tumor-permissive microenvironment. It can do so through various pathways, both intracellularly and extracellularly, as discussed in Chapter 1. Our lab previously aimed to learn whether abrogation of galectin-3 in the tumor microenvironment would allow improved antitumor T cell function. To do this, our lab used HER-2/Neu transgenic (Neu-N) mice, which are engineered to express pre-oncogenic rodent Neu (*Erbb2*) via the mouse mammary tumor virus (MMTV) promoter, leading to expression of pre-oncogenic Neu in the mammary fat pad. As they reach an advanced age, these mice grow spontaneous breast tumors due to immune self-tolerance of the Neu antigen (46).

To investigate antitumor immune responses in this model, my colleagues implanted a Neu-expressing tumor cell line in the mammary fat pad of 6-12 week old female NeuN mice and allowed it to grow until palpable. Mice then underwent a three-day treatment course including a single dose of cyclophosphamide to deplete T-regulatory cells, irradiated whole-cell Neu-directed tumor vaccine to activate DCs and induce presentation of the Neu antigen (47), and adoptive transfer of CD8$^+$ T cells from a TCR-transgenic donor mouse expressing high-avidity anti-Neu CD8$^+$ T cells (48). For TIL studies, mice were sacrificed two weeks after tumor implantation and tumor, spleen, and lymph nodes harvested and processed for analysis by flow

cytometry (**Figure 3A**). For studies of tumor-free survival, mice were given a lower initial tumor dose and an accelerated treatment course, and were then monitored for palpable tumor growth (**Figure 3B**).

Our lab crossed the NeuN mice and the transgenic $CD8^+$ T cell donor strain to background-matched *Lgals3*$^{-/-}$ (*galectin-3* KO) animals, then compared $CD8^+$ T cell effector response as indicated by duration of tumor-free survival and cytokine production by TILs. Interestingly, galectin-3 abrogation was correlated with larger percentages of TILs retaining their antitumor effector potential, as indicated by expression of interferon-gamma (IFNγ) and Granzyme B, but only when galectin-3 was abrogated in both the tumor-bearing Neu-N mouse and the transgenic T cell donor mouse (20). This indicated that galectin-3 is capable of antitumor $CD8^+$ T cell suppression, and that both the tumor-supportive microenvironment and the transgenic $CD8^+$ T cells themselves could serve as sources of suppressive galectin-3. These findings were borne out in tumor-free survival experiments, where ninety percent of *galectin-3* KO NeuN mice receiving *galectin-3* KO $CD8^+$ T cells with treatment were tumor-free sixty days after tumor implantation, but only fifty percent of normal Neu-N mice receiving normal transgenic T cells remained tumor-free at the same time point. These data taken together showed that galectin-3 is capable of antitumor $CD8^+$ T cell suppression, and that this suppression leads to impaired ability to prevent tumor escape of immune control.

The question then turned to how galectin-3 accomplished this suppression. Our lab has shown that high levels of galectin-3 can be detected on the surface of adoptively-transferred high-avidity $CD8^+$ T cells that have trafficked into the tumor

Figure 3: Timeline of NeuN tumor-infiltrating lymphocyte and tumor-free survival experiments. To study the dynamics of antigen-specific T cell responses in the NeuN mouse model and their effect on tumor-free, survival, we use two different experimental timelines. A. For tumor-free survival, mice were given the minimal tumorigenic dose of NT2.5 Neu-expressing tumor cells followed on days 2, 3, and 4 post-injection with single-dose cyclophosphamide, 3T3neuGM Neu-directed tumor vaccine, and adoptive transfer of high-avidity Neu-specific $CD8^+$ T cells respectively. B. For tumor-infiltrating lymphocyte (TIL) analysis, mice were given a larger tumor dose and palpable tumors were verified. On days 7, 8, and 9 post-injection, the same three-day treatment course was given with a higher dose of high-avidity Neu-specific $CD8^+$ T cells.

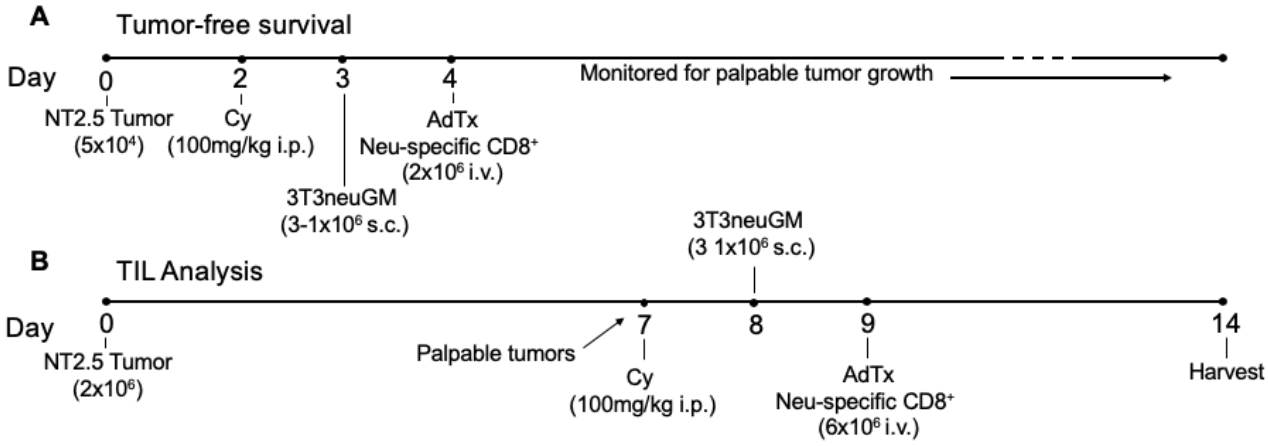

(tumor-infiltrating lymphocytes; TILs), but only low levels of surface galectin-3 are seen in the same cell population when it remains in the spleen or the tumor-draining lymph node (20, Figure). In separate experiments using healthy donor human $CD8^+$ T cells and recombinant human galectin-3, our lab has shown that the addition of exogenous galectin-3 to the culture medium during *in vitro* T cell stimulation impairs their production of IFNγ (20). Taken together, these data imply that galectin-3 may be exercising its suppressive function on $CD8^+$ T cells through a direct surface interaction, rather than through an intracellular mechanism or by mediating an effect through another cell type. Indeed, our lab has shown by Co-IP studies that galectin-3 can interact with the checkpoint molecule LAG-3 on the $CD8^+$ T cell surface. My colleague had proposed the model that secreted galectin-3 could bind LAG-3 at the $CD8^+$ T cell surface, undergo oligomerization and lattice formation, and cause LAG-3 clustering, transducing inhibitory signals into the $CD8^+$ T cell through an aberrant mechanism (20). Our lab's previous attempts to prove this mechanism downstream of LAG-3 have failed on a technical level, but the model remains a compelling hypothesis.

Galectin-3 canonically binds beta-galactoside carbohydrate residues, particularly N-acetyllactosamine, which occur ubiquitously in the N- and O-linked branched oligosaccharides found on cell surface glycans (13,14). Additionally, it is known that the pressures of the tumor microenvironment can reprogram the cells present within it, including infiltrating immune cells (49,50). These reprogramming events have huge impacts on cellular metabolism, and can lead to changes in expression and activity of enzymes that control cell surface glycosylation (51,52).

Some of the glycosylation changes that occur within the tumor microenvironment could significantly impact the ability of galectin-3 to bind cell surface glycans. While the connection between galectin-3 and LAG-3 is compelling, the ubiquity of galectin-3's canonical ligand and the potential for altered glycosylation on tumor-infiltrating immune cells makes it unlikely that this would be its only avenue of $CD8^+$ T cell suppression. I therefore first aimed to perform a survey of possible galectin-3 binding partners on the surface of $CD8^+$ TILs, and whether these binding events were facilitated more by protein expression or by altered glycosylation in a tumor context.

When my plans to interrogate the binding partners of galectin-3 on the surface of tumor-infiltrating $CD8^+$ T cells proved unattainable, I decided to pursue an avenue of inquiry more within my range of expertise. I turned to the molecular properties of galectin-3 itself, and how these could impact its ability to suppress T cell effector function. Galectin-3 binds its beta-galactoside ligand through its CRD. It also oligomerizes with other galectin-3 molecules through its NTD, as discussed in Chapter 1. While it is clear that galectin-3 has a suppressive effect upon tumor-infiltrating $CD8^+$ T cells, and seems likely that this suppression may occur through a binding event at the T cell surface, it is unclear how the dual binding domains of galectin-3 influence its ability to suppress. I therefore decided to investigate the biochemical properties of galectin-3, aiming to develop an *in vitro* system to model its suppression of tumor-infiltrating $CD8^+$ T cells, and using this system to learn how its binding properties contribute to its suppressive capabilities.

Experimental Design

To survey the glycan binding partners of galectin-3 on the TIL surface, I prepared whole cell protein lysates from freshly-isolated C57Bl/6 wildtype mouse T cells to use in the optimization of my assay, a lectin blot modeled after a standard Western blot. In this procedure, protein samples are prepared from lysates and run on a protein gel, then transferred to a membrane as with a Western blot. After blocking of the membrane, it is first incubated with recombinant mouse galectin-3, followed by anti-galectin-3 primary antibody and an HRP-conjugated secondary antibody. My intent was to prepare membrane protein extracts from adoptively-transferred transgenic $CD8^+$ T cells from either the spleen, lymph node, or tumor of our NeuN mouse model of tumor tolerance, and to compare the lectin blot band pattern seen in each sample to determine whether trafficking into the tumor microenvironment altered the cohort of galectin-3 binding partners in the assay.

My next goal was to design an assay to identify these protein binding partners. Using the lectin blot for this purpose would have been technically challenging as it would have required precisely cutting bands from a protein gel and preparing those samples for mass spectrometry to determine the identity of the proteins involved. I therefore worked to design a pull-down assay, similar to an immunoprecipitation, where a labeled recombinant galectin-3 would be added to membrane extracts from the cell populations described above. A bead-conjugated antibody to the label would be added, and binding partners could be eluted from galectin-3 using excess lactose. The goal of this approach was first to identify the binding partners of galectin-3 on TILs as opposed to T cells remaining in the spleen or lymph nodes, and then to focus on

these proteins, determining whether their expression is upregulated upon entry into the tumor microenvironment, or whether they undergo changes in glycosylation due to the metabolic effects of tumor infiltration. Through these studies, I hoped to learn what candidate proteins might mediate galectin-3 suppression of $CD8^+$ TILs, whether these proteins become binding targets by differential expression or differential glycosylation, and then to use these answers to elucidate the mechanism of suppression. It also would allow us to propose novel avenues for targeting galectin-3 in the tumor microenvironment, and could eventually lead to therapies that cause tumors to be more susceptible to immunotherapy.

To investigate how the dual binding domains of galectin-3 impact its ability to suppress $CD8^+$ T cells in a tumor context, I used an expression vector previously made in our lab containing mouse galectin-3 fused to a secretion sequence, under transcriptional control of the CMV promoter (pcDNA3.3-mGal3S). I used site-directed mutagenesis to create three mutant versions of this plasmid: a point mutant of the carbohydrate recognition domain (CRD) which should not be able to bind beta-galactoside carbohydrate residues, a truncation mutant missing the N-terminal domain (NTD) which should not be able to oligomerize, and a double mutant. For the CRD point mutant, I chose Arginine 176, a key player in the binding of beta galactosides in the CRD cleft. Initially I mutated this residue to Glycine (R176G). For the NTD truncation mutant, I engineered a version of the vector that deleted every N-terminal residue of galectin-3 up to the CRD, excepting the secretion sequence.

I had previously utilized the bacterium *Escherichia coli* (*E. coli*) for the production of recombinant galectin-3, but later found that it was impossible to fully

remove lipopolysaccharide (LPS), otherwise referred to as endotoxin, from the purified protein. I confirmed this issue in the literature (53), and learned that since galectin-3 naturally binds to LPS, full removal of endotoxin is not possible from such samples. This is also an issue with commercially-available recombinant galectin-3, which is generally produced in *E. coli*. I therefore chose to optimize a mammalian system for recombinant protein production by transiently transfecting HEK-293T cells with normal galectin-3 or mutant forms. The secretion sequence engineered onto the galectin-3 N-terminus forces secretion of the majority of recombinant protein, causing it to undergo all physiologically relevant posttranslational modifications, and allowing it to be purified from the cell culture supernatant for use in *in vitro* assays. Verification of galectin-3 secretion into the cell culture supernatant was performed by Western blot, comparing supernatant samples to 293T whole-cell protein lysates.

To purify recombinant galectin-3 from cell supernatants requires a multi-step process. The process begins with ammonium sulfate precipitation of galectin-3 directly from the culture supernatant. The protein pellets produced by precipitation are re-solubilized in protein buffer and subjected to size exclusion chromatography. The relevant fractions then go through ion exchange chromatography, beginning with anion exchange and followed by cation exchange. At each step, the fractions containing galectin-3 are verified by Western blot and passed to the next purification step. Once ion exchange is complete, galectin-3 purity is established by overloading protein in one well of a gel and staining the gel for total protein to determine whether any other contaminants remain in the sample. If so, ion exchange steps can be repeated as necessary.

While optimizing protein purification protocols, I looked for an assay to test activity of recombinant galectin-3 in an *in vitro* system. My goal was to model the activity of adoptively transferred high-avidity donor T cells in our NeuN system. In the mouse model, these naïve cells are adoptively transferred by intravenous injection, where they can then traffic to the lymph node and become primed by dendritic cell populations induced by the Neu-directed tumor vaccine. Over the next few days, these T cells travel to the tumor site, where they are re-stimulated by their cognate antigen on tumor cells, produce effector cytokines, and attempt tumor cell killing. I felt that the best way to model this initial priming and reactivation was to perform the initial priming *in vivo*, isolate the activated cells from the mouse, and perform an *in vitro* re-stimulation to assess the effector potential these T cells would have if they were trafficking to a tumor site. Our lab developed such a protocol for past assessments of previously *in vivo* activated T cells, and I used this with some modification.

This protocol uses the same transgenic $CD8^+$ T cells we examine in the NeuN model, adoptively transferred into wildtype FVB/N mice. The mice received the Neu-directed tumor vaccine utilized in the NeuN model, concurrently with the adoptively-transferred naïve T cells, and activation was allowed to proceed *in vivo* for 7 days. At this time point, I harvested spleen and lymph nodes from these mice and proceeded with a pan-T cell isolation. Isolated T cells, which included both the adoptively transferred transgenic $CD8^+$ T cells and endogenous FVB/N T cells, were then plated with T2-D^q cells, a TAP-deficient human cell line engineered for surface expression of empty mouse H2-D^q MHC class I. For this experiment, these cells were pulsed with the Neu antigenic peptide for antigen-specific re-stimulation of adoptively-transferred

transgenic T cells. The re-stimulation was performed by co-culturing isolated T cells with pulsed and washed T2-D^q cells for six hours in T cell medium containing monensin, and was followed by surface staining and intracellular cytokine staining (ICS) for flow cytometry, to assess the effector potential of the adoptively-transferred $CD8^+$ T cells after *in vivo* activation. This re-stimulation step is meant to model the re-activation of $CD8^+$ T cells that infiltrate tumor, but to provide an environment where we may assess the suppressive capability of exogenous galectin-3 in the absence of other suppressive factors.

I plan to add purified galectin-3 to the *in vitro* re-stimulation culture to see whether its suppressive effects manifest in lower levels of effector cytokine production. If we do see such suppression, and thereby confirm a direct suppression of T cells by galectin-3, I hope to test the suppressive capability of mutant forms of galectin-3. This may elucidate the question of whether carbohydrate binding, oligomerization, or both binding properties of galectin-3 are most essential to its suppressive effects on tumor-infiltrating $CD8^+$ T cells.

Materials and Methods

Site-Directed Mutagenesis

To achieve site-directed mutagenesis of the galectin-3 expression vector (pcDNA3.3-mGal3S), I used the Q5 Site-Directed Mutagenesis Kit (E0554, New England Biolabs). This kit requires the design of 5' to 5' back-to-back PCR primers, with specific primer design dependent on the intended mutation. For point mutations, one of the two primers carries the complementary base for the intended point mutation and should be designed to cover that portion of sequence. For deletion mutations, rather than abutting each other when annealed to template, the primers' 5' ends should directly flank the intended deletion site. For short insertion mutations, one primer will have the desired insertion sequence at its 5' end, such that the 5' end of one primer abuts the middle of the insertion primer when annealed to the template DNA. For longer insertions, each primer should carry half of the intended insertion on the 5' end with their middles abutting when annealed to the template DNA. I used the NEBaseChanger online tool for initial primer design, then checked the proposed primer sequences for redundant binding sites in the expression vector using SnapGene software. Once primer sequences were optimized, oligonucleotides were ordered from Integrated DNA Technologies, resuspended at 100uM, and diluted to 10uM for use in PCR.

The Q5 kit uses PCR with a high-fidelity polymerase to produce linear mutated vector sequences. PCR reactions were prepared as indicated in the kit manual, with 5-10 ng input DNA used per reaction. The PCR was run in a thermal cycler on the

program indicated in the kit manual, using the annealing temperature suggested by NEBaseChanger for each primer set and setting the extension time at 2 minutes per cycle to accommodate vector size. If primer sets were optimized beyond what was suggested by NEBaseChanger, optimal annealing temperature was determined using a standard gradient PCR protocol. PCR was then followed with the KLD reaction as detailed in the kit manual, which uses a kinase and ligase to circularize the vector, and contains *Dpn* I, a restriction enzyme which cleaves DNA at the site of methylated adenine in the sequence G^{m}A|TC, thereby removing all template DNA grown in a bacterial system and leaving the PCR product vectors intact. DNA prepared from bacteria transformed with plasmid PCR product was used to confirm mutagenesis by Sanger sequencing performed by Hopkins Genetic Resources Core Facility (GRCF).

Bacterial Transformation, Plating, Culture Growth, and Storage

I performed all transformations using chemically-competent TOP10 *E. coli* (C4040, Invitrogen) with either the standard or quick transformation protocols. I plated transformants on Luria Broth (LB) agar plates containing Ampicillin (Amp) for antibiotic selection of transformed colonies. I picked five colonies from each plate to seed 5 mL LB-Amp bacterial cultures for glycerol stocks and minipreps of plasmid DNA. I prepared glycerol stocks by mixing 500 µL bacterial culture with 500 µL 20% glycerol, then stored these at -80ºC. I used the remainder of each culture in the QIAprep Spin Miniprep Kit (27104, QIAGEN) to extract plasmid DNA, which was diluted to prepare for sequencing. After sequence verification, I used glycerol stocks of verified clones to seed 5 mL LB-Amp cultures, which were then used to seed 150 mL LB-Amp

cultures. I spun down the large cultures in 200 mL plastic centrifuge bottles to obtain pellets, which were then used in the ZymoPURE II Plasmid Maxiprep Kit (D4202, Zymo Research) to prepare maxipreps of low-endotoxin plasmid DNA. All plated cultures were incubated overnight in a 37ºC cabinet incubator. All liquid cultures were incubated overnight in a 37ºC shaking incubator at 200 rpm.

Transfection of HEK-293T Cells

Low passage number HEK-239T cells were thawed from lab freezer stocks and brought up in T175 flasks containing Complete DMEM (Dulbecco's Modified Eagle's Medium supplemented with 10% FBS Benchmark, 1% L-Glutamine, and 0.5% Penicillin-Streptomycin). When cells reached 90% confluence, the culture medium was removed and the cell bed was washed with cold 1X phosphate-buffered saline (PBS). PBS was removed by aspiration and 5 mL 0.25% Trypsin was added. Cells were trypsinized for 1 minute at 37ºC. After trypsinization, I harvested the cells using 20 mL Complete DMEM and centrifuged for 5 minutes at 4ºC, 1500 rpm. Cells were resuspended and counted, then resuspended in antibiotic-free DMEM (as above without Penicillin-Streptomycin) at a concentration of $5x10^5$ cells per 1 mL of medium. The desired amount of cell suspension was then plated in an appropriately sized container for transfections the following day.

On the day of transfection, confluence of 70-90% was confirmed, then cell culture medium was changed from antibiotic-free DMEM to Low-Serum DMEM (Dulbecco's Modified Eagle's Medium supplemented with 2.5% FBS and 1% L-Glutamine). Cells remained in the incubator during transfection preparation. All

transfections were prepared using a standard Lipofectamine 3000 protocol, where for every $1x10^6$ transfected cells,125µL Opti-MEM was mixed with 3.75 µL Lipofectamine 3000 and 125 µL Opti-MEM was mixed with 5µg of transfection vector DNA and 10µL P3000 reagent. The two transfection mixes were combined and incubated for 10 minutes at room temperature before being added to the culture medium of the transfected cells and mixed gently to incorporate. Transfections were left for 48-96 hours before beginning protein purification from cell supernatants.

Preparation of Protein Samples for Lectin Blot

To prepare lysates for lectin blot optimization, $CD8^+$ T cells were isolated from cell suspensions prepared from C57Bl/6 mouse pooled spleen and lymph nodes. IP Lysis Buffer was prepared by supplementation of Pierce Co-IP Lysis Buffer (87788, Thermo Fisher) with phenylmethylsulfonyl fluoride (PMSF), dithiothreitol (DTT), and a protease inhibitor cocktail (118361530001, Roche). 400 µL of supplemented lysis buffer was added to a cell pellet of $1.75x10^7$ $CD8^+$ T cells and pipetted up and down to resuspend. This suspension was incubated on ice for 30 minutes. Cells were them subjected to two rounds of sonication for 8 seconds each with a 30 second rest on ice in between. Lysates were centrifuged for 15 minutes at 14,000 x g in a 4ºC benchtop microcentrifuge. The supernatant was collected as the final protein lysate.

Lysate was diluted 1:5 in diH_2O, then 35µL diluted lysate was added to 12.5 µL 4X Sample Buffer and 2.5 µL 20X Reducing Agent and pipetted up and down to mix. Samples were boiled for 10 minutes at 100ºC, then cooled to room temperature and centrifuged before gel run.

Preparation of Protein Samples for Western Blot

To test for expression and secretion of transfected protein, transfected cell supernatants and pellets were harvested in parallel. Protein input was normalized by dividing total supernatant volume by total number of cells counted. A known number of cells was pelleted to make protein lysates, and a corresponding proportion of supernatant was used as input for protein samples.

To make protein samples from lysates, cells were pelleted, then lysed directly by resuspension in 1X Laemmli Sample Buffer. To make protein samples from supernatant, the appropriate supernatant volume was mixed with 5X Laemmli Sample Buffer (60 mM Tris-HCl pH 6.8, 2% sodium dodecyl sulfate, 10% glycerol, 5% beta mercaptoethanol, 0.01% bromophenol blue) and water as necessary to achieve a 1X buffer concentration. After sample preparation, all protein samples were boiled for 5 minutes at 100ºC.

Protein Gel Runs

Boiled samples were cooled to room temperature and centrifuged, then loaded into 15-well 12% Bis-Tris precast gels (NP0343, Invitrogen) with Precision Plus Dual Color Protein Standard (1610374, BioRad) used as a ladder. Gels were run at 200V in tanks containing 1X NuPage MOPS buffer (NP0001, Invitrogen) for an appropriate amount of time to allow dye migration to within 0.5 cm of the bottom of the gel.

Total Protein Staining

To detect total protein in gel run samples, gels were removed from plastic cases and rinsed in large volume (about 100 mL) diH_2O 3 times for 5 minutes each on an orbital shaker. Water rinses were discarded, then gels were submerged in 20 mL SimplyBlue Safestain (LC6060, Invitrogen) and incubated on an orbital shaker at room temperature for 1 hour.

Stain was discarded, then gels were rinsed from 3 hours to overnight in excess volume of diH_2O. This water wash was repeated 1-2 times to achieve a clear background and sharp protein gel bands. De-stained gels were imaged using a conventional flatbed scanner.

Lectin Blot for Galectin-3 Binding Partners

Gels were set up in Bio Rad Criterion transfer apparatus to transfer to nitrocellulose membrane. Transfer buffer was made fresh by combining 1.6L diH_2O, 400 mL methanol, 28.8 g UltraPure Glycine, and 6.06g Tris, and allowing to mix well on a stir plate. Transfer buffer was added to tank, and transfer run at 5V in an ice bucket in the 4ºC cold room overnight.

Transferred membranes were rinsed in fresh 1X Tris-Borate-Saline, 0.1% Tween (TBS-T) buffer for 5 minutes, then underwent blocking of nonspecific binding by incubating for one hour at room temperature in 3% bovine serum albumin (BSA) in 1X TBS-T. After blocking, buffer was discarded and recombinant mouse galectin-3 (599804, BioLegend) was added to the blot at a concentration of 0.5 µg/mL in blocking buffer and blots were incubated overnight at 4ºC.

After blocking, galectin-3 suspension was discarded and blot was washed in fresh 1X TBS-T, four times for 5 minutes each time on an orbital shaker. After washes, purified anti-galectin-3 primary antibody (125401, Biolegend) was added at a 1:1000 dilution in blocking buffer. Blot was incubated in primary antibody for one hour at room temperature on a rocker. After incubation, the four TBS-T washes were repeated.

Secondary antibody dilution was performed by adding goat anti-rat HRP secondary antibody (NA935, GE Healthcare) to blocking buffer at a concentration of 1:5000. Secondary antibody was added to blot and incubated for one hour at room temperature on a rocker, after which the four TBS-T washes were repeated.

After the final wash, blots were treated with a 1:1 mix of Pico Plus Chemiluminescent Substrate (34579, Thermo Fisher) for development. Blot was incubated for 5 minutes at room temperature, then substrate was removed for blot ECL imaging in a UVP digital imager.

Western Blot for Galectin-3 Expression

To perform galectin-3 Western blot, precast gels were removed from plastic cases and rinsed in diH_2O, then cut to size and transferred onto nitrocellulose membrane using the Invitrogen iBlot 2 dry transfer device. After transfer, membranes were trimmed and placed in a solution of 3% BSA in 1X TBS-T for blocking of nonspecific binding interactions. Blocking was performed either for one hour at room temperature or overnight at 4ºC.

After blocking, excess blocking buffer was discarded and a solution of purified anti-galectin-3 primary antibody (126701, BioLegend) diluted 1:1000 in blocking buffer

was added. Incubation was performed either for 2 hours at room temperature or overnight at 4ºC. After incubation, primary antibody solution was collected and stored at 4ºC for reuse. Blots were washed in 1X TBS-T four times for 3 minutes each on an orbital shaker.

A preparation of secondary antibody (NXA931, GE Healthcare) was made in blocking buffer at 1:20,000 concentration and added to each blot after the final wash was discarded. Incubation was performed for 1 hour at room temperature, after which secondary antibody was discarded. Blots were washed in 1X TBS-T four times for 3 minutes each on an orbital shaker.

Blots were placed in clean plastic dishes and a fresh 1:1 preparation of Pico Plus Chemiluminescent Substrate (34579, Thermo Fisher) was added for detection. Blots were incubated for 5 minutes at room temperature, then excess substrate was removed and blots were placed in plastic sheet protectors for digital imaging of ECL signal.

In the UVP digital imager, minimal exposure time was used to allow all bands present to become visible. Blot images were inverted for easier visibility of bands and any adjustments of gamma signal were performed on contiguous blots only so that band brightness was true to actual relative intensity of samples on the same blot. When images from multiple blots have been compared, exposure times have been matched and gamma adjustments have been performed in parallel.

Ammonium Sulfate Precipitation

To perform an initial purification of galectin-3, precipitation from the transfected cell supernatant with saturated ammonium sulfate solution was performed. Saturated ammonium sulfate was prepared using a standard table of mass of ammonium sulfate powder to volume of diH_2O (54). To determine the optimal concentration for precipitation of galectin-3 while leaving behind as many contaminants as possible, ammonium sulfate cuts were performed. We performed three sets of serial cuts, which involves raising the percentage of ammonium sulfate in the supernatant from zero to either 20, 30, or 40 percent. Samples were then centrifuged for 8 minutes at 17,000 x g in a benchtop refrigerated microcentrifuge at 4ºC to obtain a total centrifugation of 100,000 g-minutes.

After centrifugation, remaining supernatant was removed from the protein pellet (if any was visible) and concentration of ammonium sulfate was raised from 20, 30, or 40 percent to either 40, 50, or 60 percent. Samples were centrifuged a second time and supernatants were removed from pellets. For the final round, percentages of ammonium sulfate were raised from 40, 50, or 60 percent to 80 percent in all samples, a concentration at which nearly all protein should precipitate. Supernatant was discarded.

After cuts were performed, protein pellets were resuspended in a protein buffer containing 10 mM HEPES and 100mM sodium chloride at volumes that would normalize their protein concentration based on the volume of original cell supernatant that was used to produce each pellet. Once normalized, protein samples for gel runs were prepared as described above and gels were run for total protein assessment and

galectin-3 detection by Western blot. Galectin-3 was detected entirely in the pellet of the 30-50% ammonium sulfate cut, so for ongoing purifications, supernatant ammonium sulfate concentration was raised to 30%, allowed to equilibrate, then raised to 50% before pellet centrifugation.

Protein pellets were allowed to dry as much as possible, then were stored on wet ice at 4ºC until resuspension for chromatography column runs.

Size Exclusion Chromatography

Protein pellets were resuspended in a buffer containing 10 mM HEPES, 100 mM sodium chloride, and 20 mM lactose in milliQ diH_2O. All pellets must be resuspended at a volume not exceeding 14 mLs. After resuspension, proteins were filtered using 0.2 µm syringe filters before loading into a loop and attaching to the BioRad NGC Quest 10 chromatography system (7880001, BioRad). The protein sample was loaded onto a Hi-Prep 26/60 Sephacryl S300 size-exclusion column (17119601, GE Healthcare) previously equilibrated with the sample buffer described above, run at 1 mL per minute. Fractions were collected and total protein was assessed by SimplyBlue staining of protein gels as described above. Galectin-3 was located by Western blot.

Ion Exchange Chromatography

Pooled protein fractions from the size exclusion column run were diluted 1:5 in milliQ diH_2O to dilute sodium chloride to 20mM before loading into a loop and attaching to the chromatography system. An ENrichQ anion exchange column (780-0001,

BioRad) was equilibrated with a protein buffer containing 10mM HEPES, 20 mM sodium chloride, and 20 mM lactose. The sample was run over the column at 0.5 mL/min, with 8mL fractions collected during flow through and 1 mL fractions collected during segmented gradient elution. Fractions were collected and total protein was assessed by SimplyBlue staining of protein gels as described above. Galectin-3 was located by Western blot.

Mice

NeuN (FVB/N-Tg(MMTVneu)202Mul/J) mice were originally purchased from Jackson Laboratories and bred in-house. NeuN *Lgals3*$^{-/-}$ mice were bred as previously described (20). FVB/N background mice were purchased as needed from Jackson Laboratories. High-avidity neu-specific TCR transgenic mice (Clone100) were produced as previously described and avidity verified by tetramer staining (48). Clone100 Lagls3-/- mice were produced as previously described (20). Animals were housed in the Johns Hopkins Animal Facility and cared for according to protocols approved by the Johns Hopkins Animal Care and Use Committee.

Adoptive Transfer and Vaccine Preparation and Administration

For *ex-vivo* experiments, spleens and inguinal, axillary, brachial, and cervical lymph nodes were harvested from Clone100 mice. Organs were dissociated into single cell suspension and red blood cells were lysed, then $CD8^+$ T cell isolation was performed using a Mouse $CD8^+$ T Cell Isolation Kit (19853, STEMCELL). $CD8^+$ T cells were counted, then stained with CellTrace carboxyfluorescein succinimidyl ester

(CFSE) or CellTrace Violet proliferation dye, incubated, and washed per manufacturer's protocol. When using CellTrace Violet, one tenth of the recommended proliferation dye was used. Cells were then washed three times in 30 mL ice cold 1X PBS. On last wash, cells were counted, and the final pellet was resuspended at $1.2x10^6$ cells/mL in 1X PBS.

3T3neuGM vaccine cells or 3T3GM mock vaccine cells were cultured in CRIP VAC medium (DMEM, 10% FBS, 1% L-Glutamine, 1% non-essential amino acids, 1% sodium pyruvate, 0.5% penicillin-streptomycin, supplemented with methotrexate for selection) or CRIP MOCK medium (as above without methotrexate) until confluent. Cells were trypsinized and harvested, then counted and washed three times in ice cold 1X PBS. On the last wash cells were counted again, then resuspended at $1x10^7$ cells per mL in 1X PBS. Cells were irradiated at 50 Gy in a CIXD Biological X-Ray Irradiator (Xstrahl).

Isolated Clone100 $CD8^+$ T cells were injected intravenously into FVB/N recipients ($6x10^6$ cells per mouse in a 500 µL injection). Irradiated 3T3neuGM cells or 3T3GM mock cells were given by subcutaneous injection of 100 µL and $1x10^6$ cells into three of four limbs of each FVB/N adoptive transfer recipient.

T Cell Harvest and Re-stimulation In Vitro

To prepare the re-stimulation experiment, T2-D^q cells were cultured in EBV medium (RPMI, 10% FBS, 1% L-Glutamine, 1% non-essential amino acids, 1% sodium pyruvate, 0.5% penicillin-streptomycin, with hygromycin added for selection). Upon confluence, these cells were harvested and resuspended at $1x10^6$ cells per mL

in serum-free Complete RPMI (RPMI, 1% L-Glutamine, 0.5% penicillin-streptomycin). Neu oncogenic peptide ($RNEU_{420-429}$, PDSLRDLSVF) or control peptide ($NP_{118-126}$, RPQASGVYM) were added to the cell suspension to achieve peptide concentrations of 2.5 µg per mL of cells. Peptide pulse was performed at room temperature for at least two hours with gentle slow shaking on an orbital shaker. After pulse, T2-D^q cells were washed in Complete RPMI (RPMI 1640, 10% FBS, 1% L-Glutamine, 0.5% penicillin-streptomycin) and resuspended at $1x10^6$ cells per mL in Complete RPMI for plating in the re-stimulation.

After seven days of *in vivo* stimulaton by vaccine administration, adoptively transferred high-avidity neu-antigen-specific T cells were harvested from recipient FVB/N mice by dissecting spleens and inguinal, axillary, brachial, and cervical lymph nodes. Single-cell suspensions were prepared from organ dissociation and red blood cells were lysed. A Mouse Pan-T Cell Isolation Kit (19851, STEMCELL) was used to isolate all T cells from this suspension. Cells were counted and resuspended at $4x10^6$ cells per mL in Complete RPMI for plating in the re-stimulation.

To plate the cells for re-stimulation, 500µL of T cell suspension ($2x10^6$ cells) and 500µL of peptide-pulsed T2-Dq cells ($5x10^5$ cells) were combined in each well of a 48-well culture plate. 0.67 µL monensin (BD GolgiStop) was added to each well and each well was pipetted up and down gently to mix. Cells were allowed to undergo re-stimulation for six hours of incubation at 37ºC in a tissue culture incubator with 5% CO_2.

Flow Cytometry and Intracellular Cytokine Staining

After re-stimulation, cells from each well were harvested and spun down, then re-suspended in 100 µL PBS and plated in a 96-well V-bottom assay plate to prepare for flow cytometry staining. For viability staining, a 1:1000 dilution of Live/Dead Aqua Stain stock (L34957, Thermo Fisher) in 1X PBS was made, and all viability-stained wells were resuspended in 100 µL of this stain. Staining was performed for 30 minutes at 4ºC. Cells were washed twice in 1X PBS.

A 5 µg per mL dilution of Mouse BD Fc Block (553141, BD) was made in 1X FACS buffer (PBS, 2% FBS, 2 mM EDTA) and added to cells to block non-specific binding of fluorescent antibodies. Cells were incubated for 15 minutes at 4ºC, then washed once in FACS buffer.

Fluorescent antibody dilutions were prepared as needed and antibodies were added as single stains or cocktails to each well of cells. Surface staining was allowed to proceed for either 20 minutes at room temperature or overnight at 4ºC. Cells were washed twice in 1X FACS buffer before proceeding to intracellular stain.

To fix and permeabilize cells, all pelleted cells in the plate were resuspended vigorously in 100 µL per well of BD Fixation/Permeabilization solution (554722, BD) and incubated for 20 minutes at 4ºC protected from light. A 1X solution of BD PermWash (554723, BD) was prepared by diluting the provided reagent 1:10 in diH_2O. Cells were washed twice in 1X BD PermWash, then resuspended in 100µL per well of 1X BD PermWash for the addition of cytokine antibodies for intracellular stain. Intracellular stains were allowed to proceed for 30 minutes at 4ºC, then cells were washed twice in 1X BD PermWash, once in 1X FACS buffer, and resuspended in 250

μL per well of 1X FACS buffer for running and analysis on a Beckman Coulter Cytoflex. Appropriate single stain compensation controls, isotype antibody staining controls, and fluorescence minus one controls were included in the experiment. Flow cytometry analysis was performed with Beckman Coulter CytExpert software, and graphs of mean fluorescence intensity data were made and analyzed using GraphPad Prism software. Comparisons of mean fluorescence intensity between RNEU and NP peptide stimulations were assessed statistically using an unpaired t test with Welch's correction.

Results

Proteins Bound by Galectin-3 Are Detectable by Lectin Blot, but Complicated to Identify

To identify galectin-3 binding partners on tumor-infiltrating $CD8^+$ T cells, I wanted to develop a lectin blot assay. The lectin blot is similar to a traditional Western blot, but introduces a known quantity of a lectin of choice in place of a primary antibody. Rather than detecting a protein run on the original gel, the lectin is detected using a tag and antibody or a series of antibodies. I planned to make membrane protein extracts from adoptively-transferred tumor-infiltrating $CD8^+$ T cells to compare to adoptively-transferred cells remaining in the spleen and lymph nodes of vaccinated tumor-bearing NeuN mice, but I performed assay optimization using lysates made from the $CD8^+$ T cells of wildtype C57Bl/6 mice.

The challenge of optimizing the lectin blot was achieving a clean assay. Lectin blots traditionally utilize a tagged or biotinylated lectin so that detection may be performed with a single antibody incubation after washing excess lectin. Since this was unavailable, I used recombinant mouse galectin-3 detected with primary and secondary antibodies I had successfully used for Western blot.

I successfully optimized the lectin blot, showing that the blot results were not due to interactions of the primary or secondary antibodies with the protein sample. Unfortunately, the resulting blot showed numerous bands located in close proximity to one another (**Figure 4**). My plan for protein identification had been to run two protein gels in parallel, using one for lectin blot and retaining one from which to excise protein

Figure 4: Optimized lectin blot shows specific binding of galectin-3 to proteins present in protein lysates prepared from C57Bl/6 CD8$^+$ T cells. CD8$^+$ T cells were isolated from wildtype C57Bl/6 mice and lysates prepared from isolated cells for protein gel runs. Gels were transferred to nitrocellulose membrane and blotted with recombinant mouse galectin-3, primary anti-galectin-3 antibody, and secondary anti-rat HRP antibody. Blot was developed using ECL development reagents. Discrete bands were visualized, but could not be isolated for further downstream analysis.

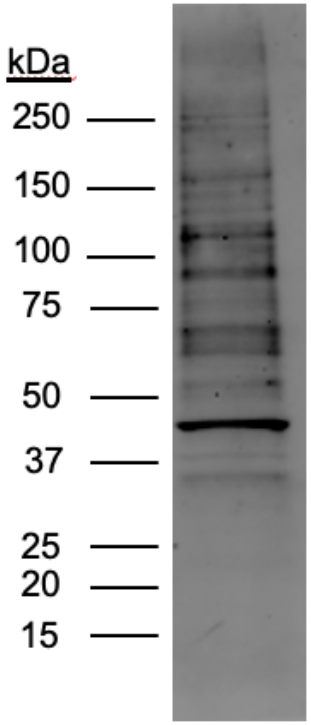

bands for identification by mass spectrometry. This was not feasible with the resulting band pattern. I needed to develop an assay that would allow a similar sampling of a protein extract without the complicating factor of excision from a gel for the identification of binding partner candidates. I therefore attempted the development of a pull-down assay similar to a conventional immunoprecipitation, but assay design failed at a technical level and I focused instead on studies of how the intrinsic properties of galectin-3 impact its suppressive functions.

Secretion of Galectin-3 Mutant Forms from Transiently Transfected HEK-293T Cells is Impaired

To test the mammalian transient transfection system, I performed small-scale transfections with the expression vectors containing galectin-3, the CRD point mutant, the NTD truncation mutant, or the double mutant. All vectors were engineered with a secretion sequence on the end coding the N-terminus of the protein to force secretion into the cell supernatant (**Figure 5A**).

When analyzed by Western blot, it became clear that the mutant forms of galectin-3 were not being successfully secreted (**Figure 5B**). While more than half of the normal galectin-3 was found secreted into the supernatant, a much smaller fraction of the point mutant was detected there. The defect was even more notable in the truncation mutant and double mutant. This was an expected outcome for the mutants truncated at the N-terminus, as this could cause the engineered secretion sequence to become buried in the globular CRD, but was an unexpected outcome for

Figure 5: Engineered expression vectors for transfection and purification of mutant forms of recombinant mouse galectin-3 show secretion defects upon transfection. A. Schematic of engineered expression vectors for forced-secretion galectin-3, the CRD point mutant, NTD truncation mutant, and double mutant. **B.** Secretion defects are seen when galectin-3 and mutant forms are detected by Western blot in transfected cell lysates or supernatants. Gel lanes shown contain protein samples made from the following transfected cell lysates or supernatants: 1, pcDNA3.3-mGal3S, with input diluted 1:10; 2, pcDNA3.3-mGal3S-tNTD; 3, pcDNA3.3-mGal3S-CRD^{R176G}; 4, pcDNA3.3-mGal3S-tNTD/CRD^{R176G}**.** Normal monomeric galectin-3 can be visualized in bands at ~29-31 kDa. Truncated galectin-3 mutants are visualized as bands at ~14-16 kD. All mutants have some defect in secretion, which is more egregious in the truncation mutants than the point mutant.

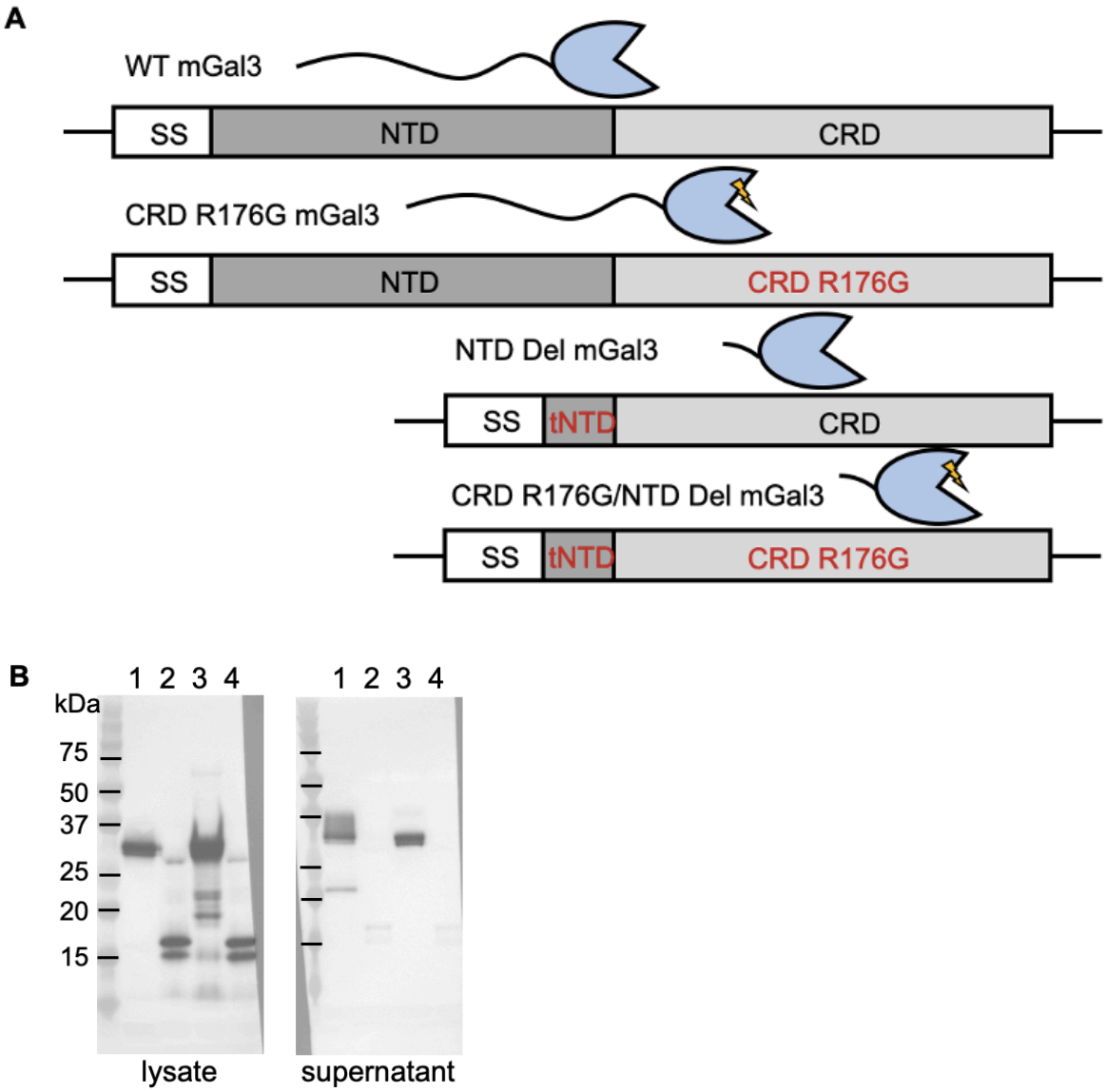
A
WT mGal3
SS
NTD
CRD
CRD R176G mGal3
SS
NTD
CRD R176G
NTD Del mGal3
SS
tNTD
CRD
CRD R176G/NTD Del mGal3
SS
tNTD
CRD R176G
B
1 2 3 4
1 2 3 4
kDa
75
50
37
25
20
15
lysate
supernatant

the point mutant, which I hypothesized would retain a similar structure and properties to those of normal galectin-3.

Transfection of Galectin-3 into HEK-293T Cells May Be Performed in Low-Serum Conditions

When developing and testing protein purification strategies for galectin-3 from the supernatant of HEK-293T cells, a major concern was the presence of protein contaminants from the cell culture medium. While it is important to purify a secreted form of galectin-3 so that it retains its pertinent post-translational modifications, the serum present in cell culture medium is one of the largest sources of protein contamination to this system. I therefore wanted to test the capability of transfected HEK-293T cells to produce recombinant galectin-3 when transfected in culture medium containing low or no added serum.

I seeded cells overnight for transfection the following morning. Directly prior to transfection, the normal transfection culture medium was removed and replaced with either fresh transfection medium (10% fetal bovine serum), 5%, 2.5%, or 0% serum medium. I performed the transfections and incubated the cells for 48 hours. After incubation, I harvested the supernatants from each transfection and prepared protein samples for galectin-3 Western blot. The blot results showed that cells transfected with galectin-3 produced equal amounts of protein as long as the culture medium contained some level of fetal bovine serum (**Figure 6**). Unsurprisingly, transfecting cells in serum-free medium caused cellular dysfunction that led to very low levels of recombinant protein being produced, but the amount of galectin-3 produced in the

Figure 6: Transfection of galectin-3 into HEK-293T cells is successful in low-serum conditions. To attempt to decrease the concentration of bovine serum albumin (BSA) in the supernatant of transfected cells, transfections (mock transfection, pcDNA3.3-EV, or pcDNA3.3-mGal3S) were performed in culture medium supplemented with either no fetal bovine serum (FBS), 2.5% FBS, 5% FBS, or 10% (normal) FBS. Protein samples for gel run were made from cell supernatants 72 hours following transfection, and were analyzed by Western blot for galectin-3. Gel lanes shown contain protein samples made from the following transfected cell supernatants: 1, mock, no FBS; 2, mock, 2.5% FBS; 3, mock, 5% FBS; 4, mock, 10% FBS; 5, EV, no FBS; 6, EV, 2.5% FBS; 7, EV, 5% FBS; 8, EV, 10% FBS; 9, mGal3S, no FBS; 10, mGal3S, 2.5% FBS; 11, mGal3S, 5% FBS; 12, mGal3S, 10% FBS. As expected, no galectin-3 was detected by Western blot for mock or empty vector transfections. Only cells grown in medium containing no FBS showed any defect in production of galectin-3. Monomeric galectin-3 is detected as a band of ~29-31kDa.

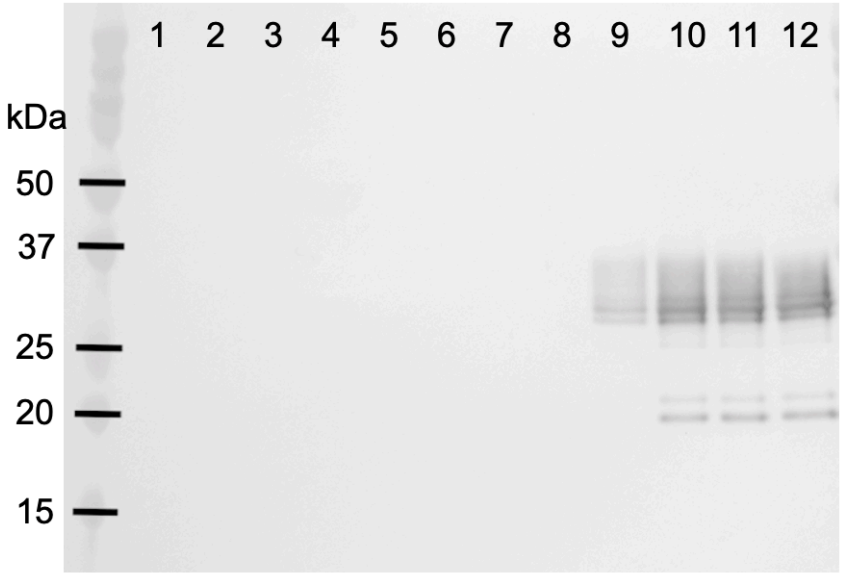

10%, 5%, and 2.5% serum conditions was very similar. Based on these data, I used 2.5% serum culture medium for all large-scale transfections used in protein purification.

Purification of Recombinant Galectin-3 Requires Excess Lactose and a Multi-Step Approach

While working to optimize the transfection and secretion of galectin-3 mutant forms, I began the process of purifying normal galectin-3 from HEK-293T cell supernatants. I began by optimizing an ammonium sulfate precipitation, to find at what percent ammonium sulfate galectin-3 precipitates relative to the bulk of protein in the cell supernatant. By testing multiple percentages, performing the precipitations, and comparing galectin-3 Western blots to total protein stains, I determined that the 30-50% ammonium sulfate fraction is optimal (**Figure 7A-B**). At this concentration, the entirety of galectin-3 is found in the protein precipitate, while a significant amount of contaminating protein remains in the supernatant, as can be seen by a serial precipitation.

I followed this with various column-based purification strategies. We began by running the resuspended pellets from ammonium sulfate precipitation over a size exclusion column in an attempt to separate galectin-3 from bovine serum albumin (BSA), the most prevalent protein contaminant in the cell culture medium. While some BSA was removed during the precipitation step, a significant amount remained in the sample. In our initial size exclusion runs, when analyzing the collected fractions by galectin-3 Western blot, we saw that much of the galectin-3 came off of the size

Figure 7: Ammonium sulfate cuts precipitate different protein fractions from transfected cell supernatants for an initial purification of recombinant mouse galectin-3. Cell supernatant was divided into three parts and the ammonium sulfate concentration raised from 0 to 20, 30, or 40 percent. These fractions were centrifuged and supernatants were removed and raised from 20, 30, or 40 percent ammonium sulfate to 40, 50, or 60 percent. Centrifugation was repeated and supernatants removed and raised from 40, 50, or 60 percent ammonium sulfate to 80 percent in each. Centrifugation was repeated a final time. Precipitated protein was resuspended in protein buffer and diluted to normalize protein input across samples before gel runs. Gels were either stained for total protein or transferred for galectin-3 Western blot. Gel lanes shown contain protein samples made from the following ammonium sulfate cut pellets: 1, 0-20%; 2, 20-40%; 3, 40-80%; 4, 0-30%; 5, 30-50%; 6, 50-80%; 7, 0-40%; 8, 40-60%; 9, 60-80%. **A.** Total protein stain. All protein remaining in lane 6 has been removed from the fraction containing galectin-3. **B.** Galectin-3 Western blot. All target protein is present in the pellet of the 30-50% fraction (lane 5).

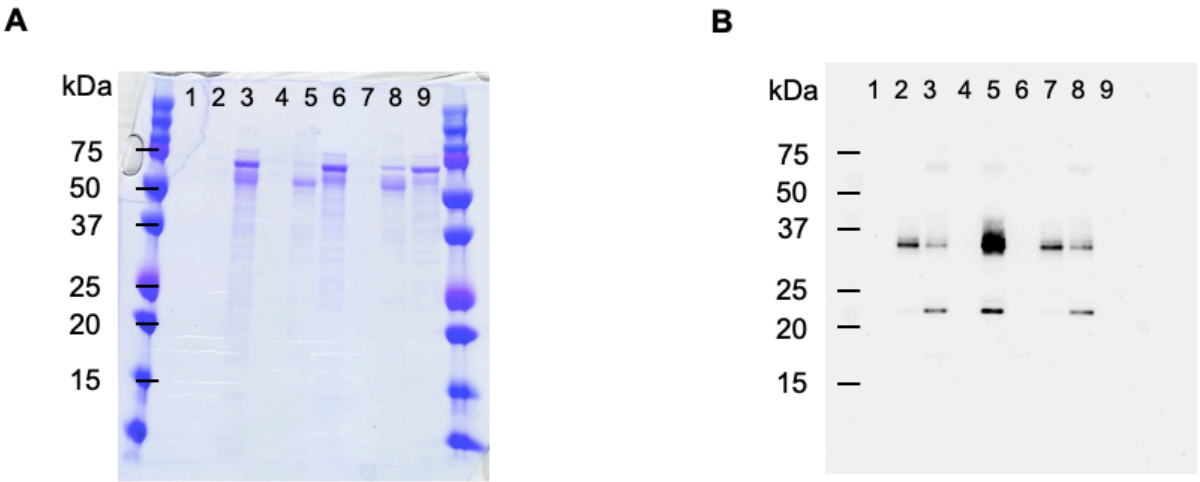

exclusion column in the same fractions as BSA, despite the size difference of these two proteins (**Figure 8A-B**). In fact, galectin-3 was leaving the column much earlier than we would expect it to, based on its size. We therefore repeated the run, but resuspended the protein pellet in a buffer containing 20 mM lactose. The same lactose buffer was used to equilibrate the column.

With the addition of excess lactose to the buffer, we saw galectin-3 separate from BSA in the column fractions and elute in fractions appropriate to its size (**Figure 8C-D**). This indicates that galectin-3 was associating with BSA, and that competitive binding with excess lactose broke the association, allowing further purification of the protein. All runs have therefore been performed in buffers containing 20 mM lactose to discourage associations with contaminating proteins.

Following size exclusion, we pooled the fractions containing galectin-3 as determined by Western blot and ran these on an anion-exchange column. Our initial run showed that galectin-3 binds Q resin, and that it may be eluted using a salt gradient (**Figure 9A**). We developed an optimized segmented gradient for elution that allowed optimal separation between galectin-3 and contaminating proteins, and showed a further improvement in separation (**Figure 9B-C**). While purification is not yet complete, this two-step column protocol after ammonium sulfate precipitation has already yielded a semi-pure suspension of galectin-3.

Figure 8: Purification by size exclusion chromatography requires excess lactose in the protein buffer to reduce binding interactions. Protein fraction purified by 30-50% ammonium sulfate precipitation was resuspended in protein buffer and run over an equilibrated size exclusion column. **A.** Chromatogram showing protein elution from the column with normal protein buffer. Boxed region shows fractions analyzed for total protein and galectin-3. **B.** Total protein stain and galectin-3 Western blot. Gel lanes are labeled with the number of the fraction being analyzed. The majority of galectin-3 is found in fractions 18, 19, and 20, which are also the main fractions containing BSA. **C.** Chromatogram showing protein elution from the column with buffer supplemented with 20 mM lactose. Blue boxed region shows fractions analyzed for total protein and galectin-3 and red boxed region shows fractions where galectin-3 was detected. **D.** Total protein stain and galectin-3 Western blot with 20 mM lactose. Gel lanes are labeled with the number of the fraction being analyzed. The majority of galectin-3 is found in fractions 21-27 while BSA is largely present in fractions 15-20.

A

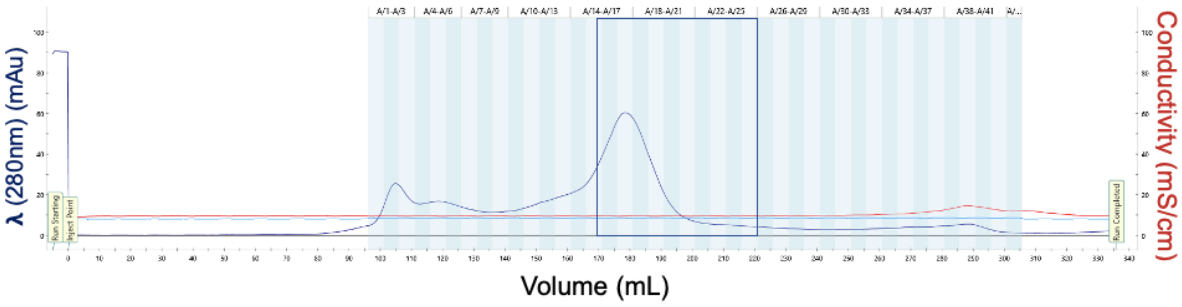
λ (280nm) (mAu)
Conductivity (mS/cm)
Volume (mL)

B

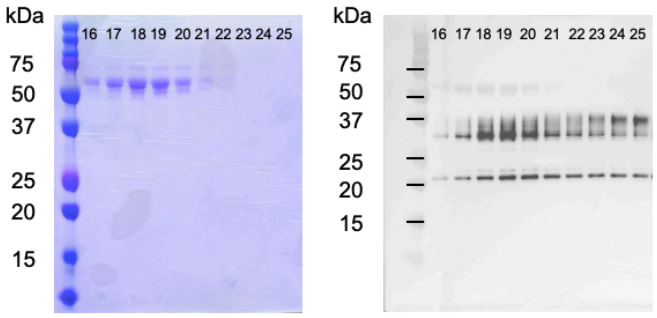
kDa
16 17 18 19 20 21 22 23 24 25
75
50
37
25
20
15
Total Protein
kDa
16 17 18 19 20 21 22 23 24 25
75
50
37
25
20
15
Galectin-3

C

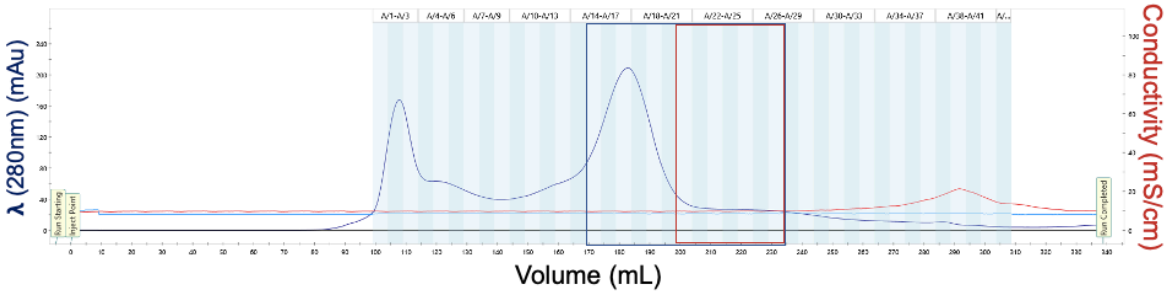
λ (280nm) (mAu)
Conductivity (mS/cm)
Volume (mL)

D

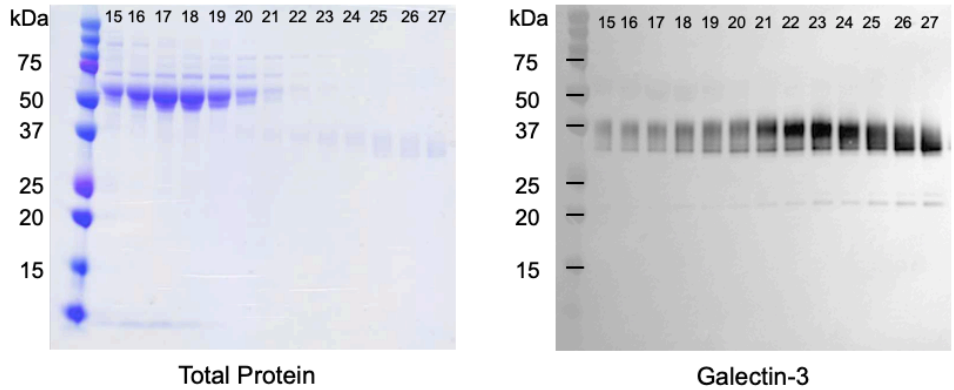
kDa
15 16 17 18 19 20 21 22 23 24 25 26 27
75
50
37
25
20
15
Total Protein
kDa
15 16 17 18 19 20 21 22 23 24 25 26 27
75
50
37
25
20
15
Galectin-3

Figure 9: Galectin-3 undergoes further purification with the use of anion-exchange chromatography and a segmented elution gradient. Protein fractions from the size exclusion column were pooled and diluted with water to decrease sodium chloride concentration, then run over a Q resin anion-exchange column and eluted with a salt gradient in buffers supplemented with 20 mM lactose. **A.** Chromatogram showing protein elution from the column with a standard salt gradient. Boxed region shows fractions containing eluted protein. **B.** Chromatogram showing protein elution from the column with a segmented gradient. Blue boxed region shows fractions analyzed for total protein and galectin-3. Red boxed region shows fractions in which galectin-3 was detected. **C.** Total protein stain and galectin-3 Western blot. Galectin-3 is detected largely in fractions 28-31, while major contaminants are found in fractions 32-39.

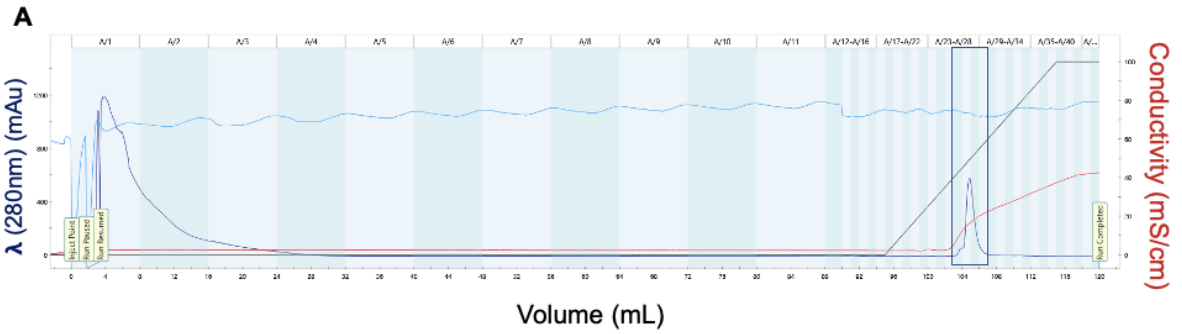
A
λ (280nm) (mAu)
Conductivity (mS/cm)
Volume (mL)

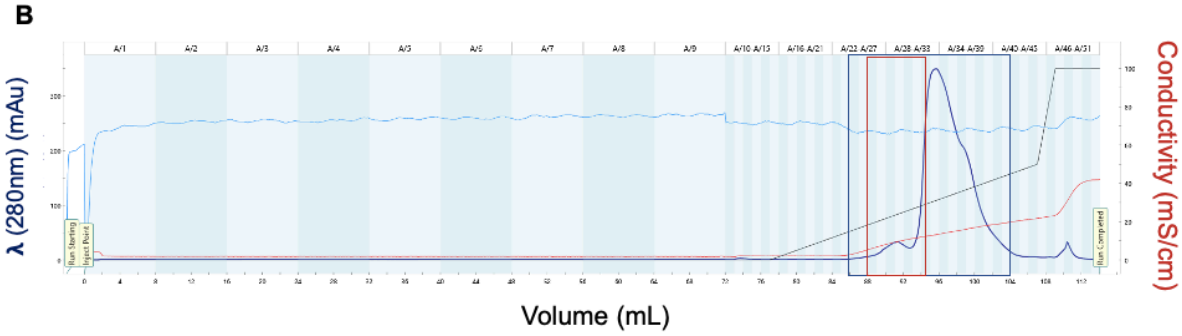
B
λ (280nm) (mAu)
Conductivity (mS/cm)
Volume (mL)

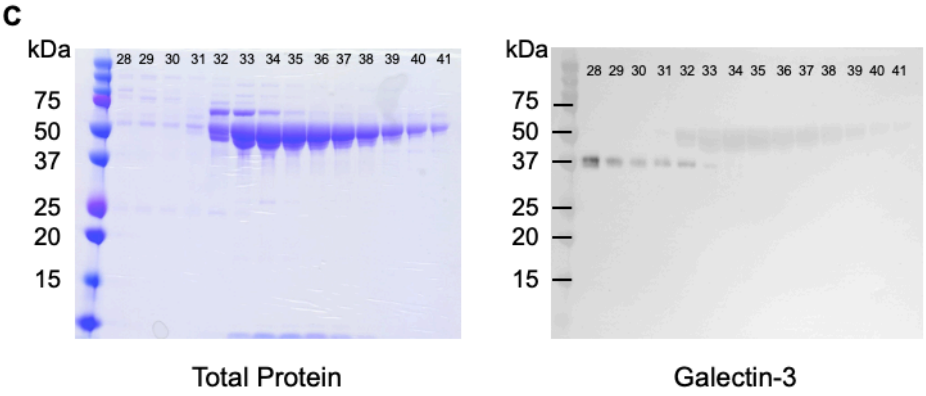
C
kDa
28 29 30 31 32 33 34 35 36 37 38 39 40 41
75
50
37
25
20
15
Total Protein
kDa
28 29 30 31 32 33 34 35 36 37 38 39 40 41
75
50
37
25
20
15
Galectin-3

Re-stimulation of Vaccine-Primed Ex Vivo *CD8$^+$ T Cells Allows Assessment of Effector Function*

To model the activation and effector response we see in our adoptively-transferred transgenic CD8$^+$ T cells in the NeuN mouse model of tumor tolerance, I utilized the *ex vivo* re-stimulation protocol developed in our lab (**Figure 10**) and described in Materials and Methods above.

It was first necessary to prove that the Neu-directed tumor vaccine was provoking the activation and proliferation of adoptively-transferred CD8$^+$ T cells *in vivo*. I was able to use our mock vaccine cell line to compare the Neu-directed vaccine to one expressing no antigen, which should not lead to proliferation and expansion of adoptively-transferred cells. All mice received adoptive transfer of Neu-specific CD8$^+$ T cells from a transgenic donor. Mice were sorted into three treatment groups, one with Neu-directed vaccine, one with mock vaccine, and one with no vaccine administered. One mouse per group was harvested at each assessed time point after dosage: 24 hours, 48 hours, 4 days, and 8 days. At the 24 and 48 hour time points, adoptively-transferred cells were detectable in all mice, and this cell population had not yet undergone any cell divisions (**Figure 11A**). At 4 days, in mice receiving adoptive transfer either alone or with mock vaccine, only trace numbers of adoptively-transferred cells were still present, and these had not undergone proliferation. In contrast, the cells in the mice receiving Neu vaccine had both proliferated and undergone several rounds of cell division (**Figure 11B**). At 8 days, no adoptively transferred cells were detectable in the mice that received transfer alone or with mock vaccine, but they remained present in the Neu vaccine mice, and all cells detected

Figure 10: An ex vivo re-stimulation assay for in vitro modeling of galectin-3-mediated suppression of CD8$^+$ T cells. Neu antigen-specific CD8$^+$ T cells are isolated from a T cell transgenic donor, labeled with proliferation dye, and adoptively transferred into an FVB/N recipient mouse on the same day as vaccination with a whole-cell irradiated Neu-expressing cell line. *In vivo* activation is allowed to proceed for 7 days. Spleen and lymph nodes are harvested for T cell isolation on day 7 and isolated total T cells are plated on peptide-pulsed T2-D^q cells. Galectin-3 or mutant protein may be added to the supernatant during a six hour *in vitro* re-stimulation in the presence of monensin. Cells are stained for surface and intracellular markers and analyzed by flow cytometry.

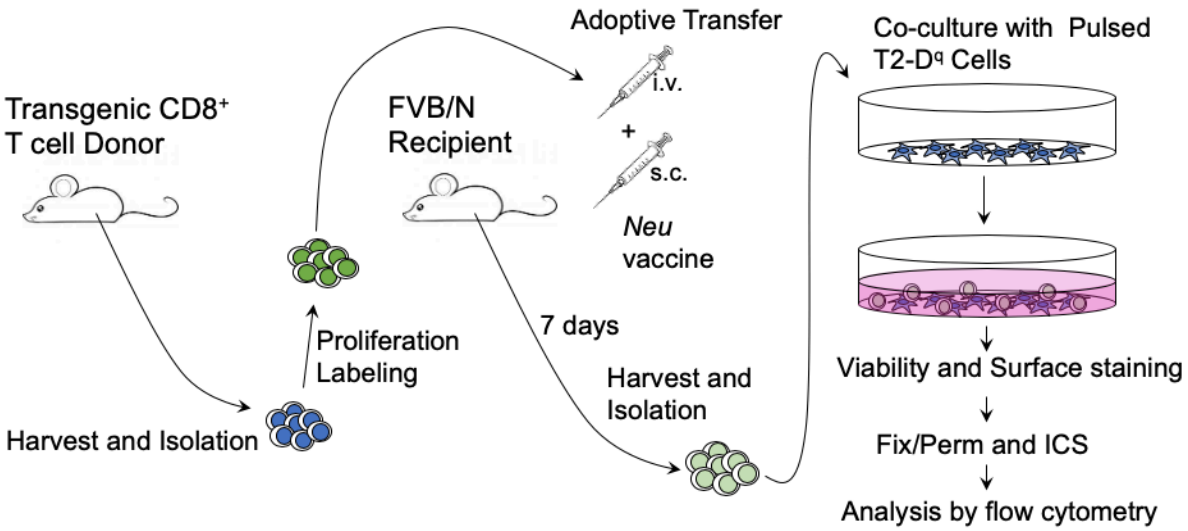

Figure 11: Adoptively transferred Neu-specific $CD8^+$ T cells activate and proliferate in response to Neu-directed vaccine but not to mock vaccine. Adoptively-transferred T cells pre-stained with CFSE were harvested from FVB/N mice 24 hours, 48 hours, 4 days, or 8 days after vaccine, mock vaccine, or no vaccine. Cells were stained directly for surface markers and analyzed by flow cytometry to assess *in vivo* proliferation. **A.** Proliferation staining on cells isolated after 24 or 48 hours *in vivo*. Adoptively-transferred cells were apparent in all three treatments and no proliferation had yet occurred. **B.** Proliferation staining on cells isolated after 4 or 8 days *in vivo*. Adoptively-transferred cells only persisted in mice that received antigen-specific vaccine. At 4 days, multiple cell divisions had occurred. By 8 days, all persisting adoptively-transferred cells had undergone activation and proliferation.

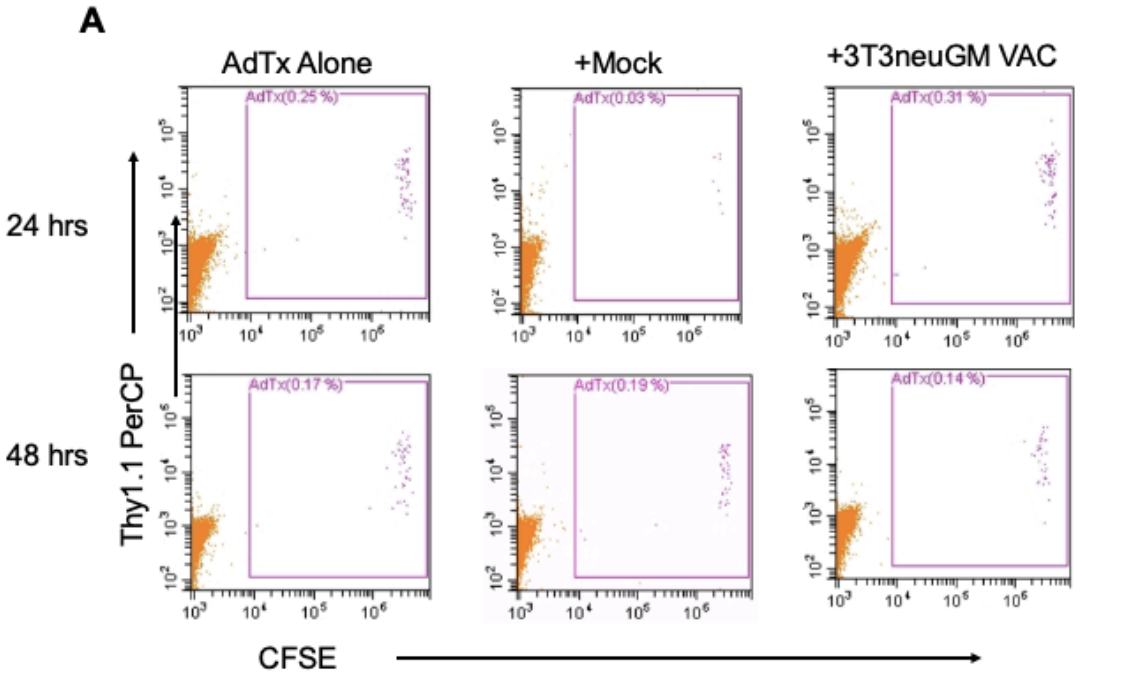
A
AdTx Alone
+Mock
+3T3neuGM VAC
24 hrs
48 hrs
Thy1.1 PerCP
CFSE
AdTx(0.25 %)
AdTx(0.03 %)
AdTx(0.31 %)
AdTx(0.17 %)
AdTx(0.19 %)
AdTx(0.14 %)

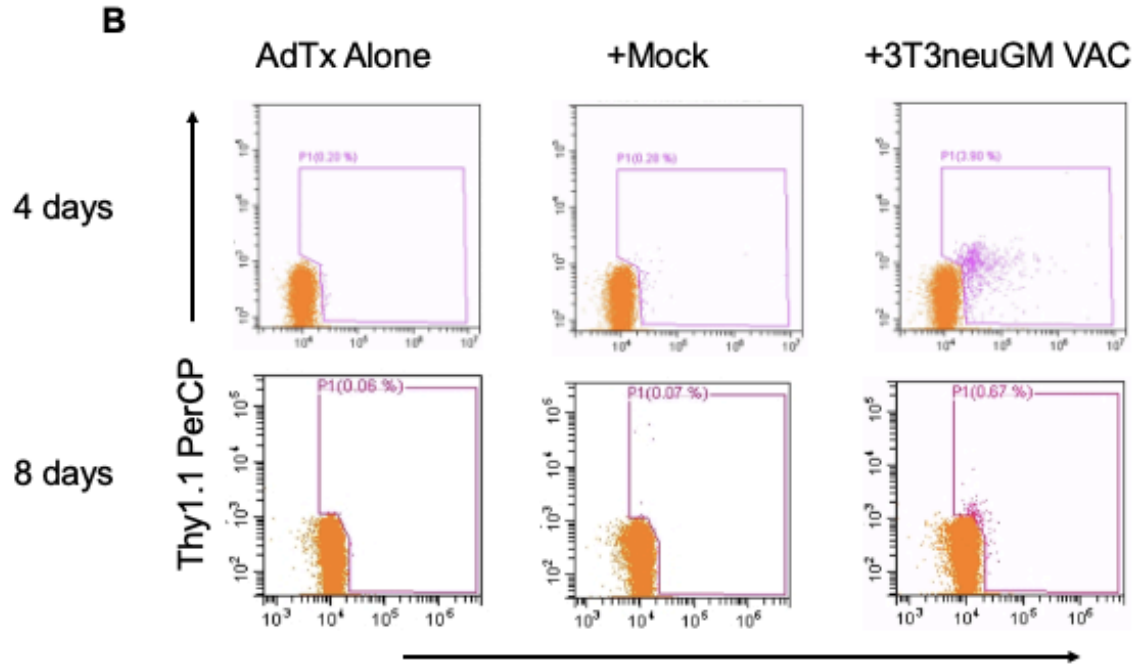
B
AdTx Alone
+Mock
+3T3neuGM VAC
4 days
8 days
Thy1.1 PerCP
P1(0.06 %)
P1(0.07 %)
P1(0.67 %)

had undergone proliferation (**Figure 11B**). This indicates that all adoptively-transferred cells harvested at this time point would be primed against the Neu antigen.

I then wanted to show that the re-stimulation of primed cells would allow us to assess these cells' capability of producing effector cytokines. Using adoptively-transferred cells harvested from mice receiving the Neu vaccine 7 days earlier, I performed the re-stimulation either by culturing isolated T cells alone, or at a 4:1 ratio with peptide-pulsed T2-D^q cells. One set of T2-D^q cells was pulsed with the Neu antigenic peptide P50, and the other with the control peptide NP. Indeed, T cells that saw their cognate peptide in culture produced easily-detectable levels of the cytokines interferon-gamma (IFNɣ), tumor necrosis factor alpha (TNFα), and interleukin-2 (IL-2), while those cultured with cells holding a control peptide did not (**Figure 12A-C**). This indicates that my assay gives a successful readout of T-cell re-stimulation after in vivo priming, and that if galectin-3 is capable of and sufficient for $CD8^+$ T cell suppression during re-stimulation, I will be able to detect it.

Figure 12: Re-stimulation *in vitro* allows detection of effector cytokines when stimulated with presentation of antigenic peptide but not with control peptide.

T cells isolated after 7 days of *in vivo* activation and proliferation were cultured on T2-D^q cells pulsed with either antigenic P50 or control NP peptide. After a six hour *in vitro* re-stimulation, cells were harvested and stained with fluorescent antibodies for surface and intracellular markers. All cells analyzed below were gated on adoptively transferred cells. Mean fluorescence intensity (MFI) is graphed in relative fluorescence units. Statistical significance was assessed using a Student's unpaired t test with Welch's correction. **A.** IFNɣ staining in cells stimulated on P50 or NP peptide-pulsed T2-D^q cells. **B.** TNFα staining in cells stimulated on P50 or NP peptide-pulsed T2-D^q cells. **C.** IL-2 staining in cells stimulated on P50 or NP peptide-pulsed T2-D^q cells.

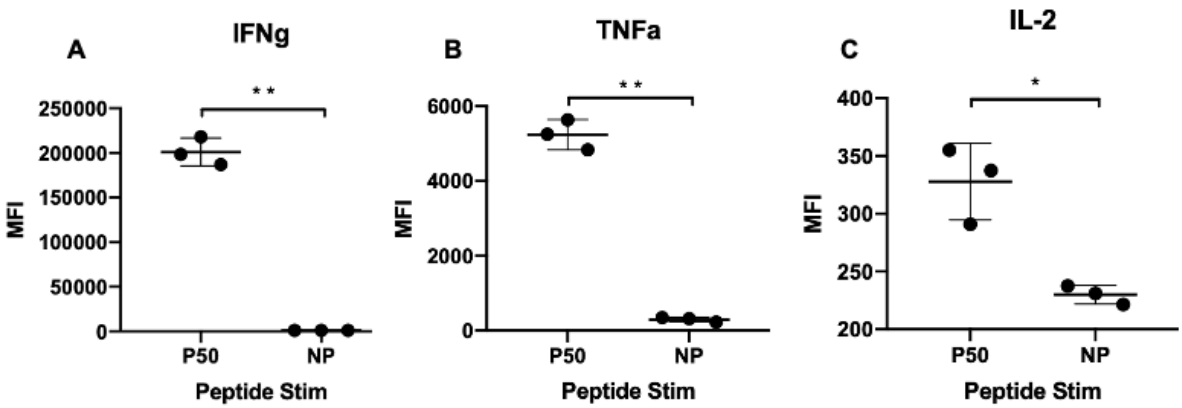

Discussion and Upcoming Work

Our lab has shown previously that galectin-3 impairs effector functions of antitumor $CD8^+$ T cells, binding directly to the cell surface and dampening the production of effector cytokines and granules by these cells in the tumor microenvironment. Removal of galectin-3 from this system results in improved production of effector molecules and longer-term immune control of tumor growth. Working off of this research, I have aimed to develop an *in vitro* system that will allow us to learn more about the mechanism of this suppressive interaction. I first attempted identification and characterization of protein binding partners of galectin-3 on tumor-infiltrating $CD8^+$ T cells, first by a lectin blot approach and then by a pull-down assay. When these avenues of inquiry proved unattainable with the methods and expertise I had available at the time, I turned to the question of how each unique binding domain of galectin-3 impacts its suppressive capability.

Using an assay modified from one our lab used previously, I have shown that antigen-specific $CD8^+$ T cells activated *in vivo* may be successfully harvested and assayed for effector potential *in vitro*. *In vivo* activation occurs specifically in response to a vaccine for the cognate antigen, and not in the presence of mock vaccine. Re-stimulation *ex vivo* successfully gives a readout of increased effector cytokine production in the presence of antigen-presenting cells bearing cognate peptide-MHC, but not with control peptide-MHC. We therefore have an established assay that will allow us to assess the effect of galectin-3 on the type of reactivation a $CD8^+$ T cell would encounter in a tumor context, without the presence of outside factors.

In my upcoming work, I will be adding exogenous galectin-3 to these re-stimulation cultures to verify the phenomenon we have seen under other experimental conditions, where we believe galectin-3 is binding directly to the T cell surface to suppress effector functions. If we see a significant decrease in the production of effector cytokines or components of cytotoxic granules upon the addition of purified recombinant galectin-3, we can be sure that suppression was not caused by confounding factors, and that the mechanism of suppression is likely to be mediated through a specific binding event at the T cell surface. Additionally, our lab already has the transgenic CD8+ T cell donor and FVB/N recipient mouse strains crossed to matched-background *galectin-3* KO strains, so we will be able to test the assay in a *galectin-3*-deficient system, where the discrepancy between effector potential at baseline and in the presence of exogenous galectin-3 may be even more stark. We may then be able to assess these differences through assays that will allow us to determine through which cellular pathways galectin-3 is working to perform its suppression.

To make the purified recombinant galectin-3 that is essential for this assay, as well as its mutant forms, I used an expression vector engineered in our lab to contain mouse galectin-3 that would be forcibly secreted from a cell transfected with the vector. I engineered mutant forms of galectin-3 by performing site-directed mutagenesis to make a CRD point mutant, an NTD truncation mutant, and a double mutant. I also optimized a mammalian transfection system using HEK-293T cells in order to have an endotoxin-free purified protein fraction with all relevant post-translational modifications. Upon transfection of the three mutant proteins, however,

we found significant problems with each. All three showed secretion defects and were not detected in the cell supernatant at high levels. For the truncation mutants this was not surprising- the N-terminal secretion sequence may have been buried within the folded CRD and been inaccessible. It was more surprising for the CRD point mutant, which displayed an entirely different pattern of expression in the transfected cell lysate and supernatant than normal galectin-3 did. I hypothesize that mutating the key Arginine residue to Glycine may have caused a defect in protein folding that altered the properties of the mutant protein, causing changes in binding affinities and leading to altered expression.

To attempt to remedy the secretion defects seen in the mutant proteins, I aim to engineer new galectin-3 mutants. For my point mutant, I will be mutating Arginine 176 to Leucine, a branched nonpolar amino acid which may allow for less structural change than Glycine while also abrogating Arginine's positively-charged side chain. For the truncation mutants, I plan to make new versions that retain a section of the galectin-3 NTD. By allowing some space between the CRD and the secretion sequence, I hope to see these proteins present at higher proportions in the cell supernatant. Once these mutagenesis steps are complete, the vectors may be tested in the transfection system and compared to the previous mutants and to normal galectin-3.

The purification of recombinant galectin-3 is nearing completion. By showing that transfection is successful in low-serum conditions, I was able to remove a large part of the contaminating BSA fraction before purifications begin. We have already optimized ammonium sulfate precipitation, size exclusion chromatography, and anion-

exchange chromatography, and learned that using excess lactose in our running buffers discourages galectin-3 from undesired associations with contaminants. Our upcoming plan is to use this workflow followed with a cation-exchange chromatography step, then to begin assessments of protein purity. This will be achieved by loading a concentrated protein sample onto a denaturing protein gel and staining for total protein. We may then assess what percentage of total protein present in the fraction is galectin-3, and what proportion is contaminating protein. Depending on what contaminants remain, we will decide which column runs to repeat as part of our finalized workflow. Once this is complete, we will have pure mouse galectin-3 to use in the *ex vivo* $CD8^+$ T cell re-stimulation assay.

While the answer to the question of how the binding properties of galectin-3 impact its ability to suppress $CD8^+$ T cells remains open, the development of an assay and appropriate reagents to test the mechanism of suppression in vitro brings us one step closer to learning more about this interaction. The largest remaining obstacle will be the purification of mutant forms of galectin-3, which may have vastly different properties from the normal protein. It is my opinion that this pursuit is worthwhile due to its potential to point us to a specific mechanism of galectin-3-mediated suppression of antitumor T cells.

CHAPTER 4: An Unexplained Link Between Galectin-3 and Antigen-Presenting Cells

Rationale and Experimental Design

In our previous studies of the impact of galectin-3 on effector functions of $CD8^+$ T cells, our lab also investigated other immune cell types in the normal NeuN mice compared to *galectin-3* KO mice. As discussed in Chapter 1, previous research has shown mechanisms of immune suppression mediated by dendritic cell (DC) and plasmacytoid dendritic cell (pDC) dysfunction. Interestingly, my colleague found that the numbers of plasmacytoid dendritic cells (pDCs) in *Lgals3*$^{-/-}$ (*galectin-3* KO) NeuN mice were significantly higher than in normal NeuN mice, even before the implantation of tumor or the administration of a treatment course. My colleague's interpretation of this information was that the loss of galectin-3 causes a sharp increase in pDC numbers above baseline (20). I wanted to test this interpretation, and to learn more about its implications regarding immune modulation in the tumor microenvironment by galectin-3.

To verify what my colleague had seen, I used tumor- and treatment-naïve normal NeuN female mice age-matched to their *galectin-3* KO counterparts. I harvested lymph nodes from these mice, prepared single-cell suspensions, and stained with fluorescent antibodies for the pDC markers Ly6C, B220, and CD11c. I then analyzed these cells by flow cytometry to determine whether I saw the same discrepancy in cell numbers.

Following this inquiry, I wanted to learn whether this discrepancy in pDC numbers is a commonality seen in many mouse strains upon abrogation of galectin-

3. Our lab maintains breeding stocks of *galectin-3* KO mice in the background strains FVB/N and C57Bl/6, so I performed the experiment described above comparing these strains to their wildtype counterparts as well. I also examined pDC numbers in compartments other than the lymph nodes, examining spleens and blood to see whether the observed increase in lymph node pDCs was actually due to a shift in localization of these cells from one compartment to another.

Finally, I wanted to learn whether other mouse models of cancer might demonstrate a difference in pDC numbers upon galectin-3 abrogation. For this reason, I compared pDC numbers at baseline in the lymph nodes of KPC and KPC-G mice to those I see in NeuN or *galectin-3* KO NeuN mice.

Materials and Methods

Mice

FVB/N background mice were purchased as needed from Jackson Laboratories. FVB/N *Lgals3*$^{-/-}$ (*galectin-3* KO) mice were bred and backcrossed as previously described and bred in-house. NeuN (FVB/N-Tg(MMTVneu)202Mul/J) mice were originally purchased from Jackson Laboratories and bred in-house. NeuN *galectin-3* KO mice were bred as previously described. C57Bl/6 and C57Bl/6 *galectin-3* KO mice were purchased from Jackson Laboratories and bred in-house. KPC and KPC-G mice were produced as described in Chapter 2. Animals were housed in the Johns Hopkins Animal Facility and cared for according to protocols approved by the Johns Hopkins Animal Care and Use Committee.

Isolation of Total Cell Suspension from Spleen and Lymph Node

Target mice were sacrificed and spleen and/or lymph nodes dissected. Organs were placed into 100μM cell strainers inside of 6 well culture dishes containing 5mL per well of Complete RPMI (RPMI 1640, 10% FBS, 1% L-Glutamine, 0.5% penicillin-streptomycin). To dissociate into single-cell suspension without damaging dendritic cell populations, spleens were first chopped into small pieces in a petri dish using a razor blade, then returned to the cell strainer, where the plunger of a 3mL syringe was used to press pieces gently against the mesh until all material but connective tissue had passed through. Lymph nodes were placed directly into cell strainer and gently pressed against the mesh until all material but connective tissue had passed through. Single-cell suspensions were subjected to red blood cell lysis, centrifuged, then

resuspended in Complete RPMI and passed through a new 100μM cell strainer to filter out dead material from lysis. Cells were counted, centrifuged, then resuspended at $1x10^7$ cells per mL in 1X PBS for flow cytometry staining.

Isolation of Non-Erythrocyte Cell Fraction from Blood

Large-volume blood samples were collected from target mice by clipping of the vena cava immediately after euthanasia. Blood was pipetted into tubes treated with 0.5M EDTA to prevent clotting, then centrifuged. Red blood cell lysis was performed and cells were centrifuged, then resuspended in Complete RPMI and passed through a 100uM cell strainer to remove dead material from lysis. Cells were counted, then centrifuged and resuspended at $1x10^7$ cells per mL in 1X PBS.

Flow Cytometry

Cell staining began by pipetting cells into a 96-well V-bottom culture plate and pelleting by centrifugation. All wells to be stained for viability were then resuspended in 100 μL of a 1:1000 dilution of Live/Dead Aqua stain stock solution in 1X PBS. Staining was performed for 30 minutes at 4°C. After staining, 100 μL 1X PBS was added to each well before centrifugation. Cells were washed an additional two times with 1X PBS.

Each well was then resuspended in 100 μL of Mouse BD Fc Block diluted to 5 μg per mL in 1X FACS buffer (1X PBS, 2% FBS, 2 mM EDTA) and plate was incubated at 4°C for 15 minutes.

After incubation with Fc Block, fluorescent antibodies for surface staining were added directly to wells as appropriate to achieve desired dilutions. Staining was performed either for 20 minutes at room temperature or overnight at 4°C, protected from light.

After staining, samples were washed twice with 1X FACS buffer, then analyzed on a Beckman Coulter Gallios. Appropriate single stain compensation controls, antibody isotype controls, and fluorescence minus one controls were included.

Results

Plasmacytoid Dendritic Cell Numbers are Lower in Normal NeuN Mice Than in Matched Galectin-3 KO NeuN Counterparts

When comparing pDC numbers in NeuN mice compared to their *galectin-3* KO counterparts, I saw the same phenomenon described by my colleague, where pDC numbers were much higher in *galectin-3* KO animals than in normal NeuN mice (**Figure 13A**). To elucidate this finding, I repeated the experiment to compare these numbers in the NeuN background strain, FVB/N. Wildtype FVB/N mice have, on average, the same number of pDCs in their lymph nodes as their matched *galectin-3* KO FVB/N counterparts (**Figure 13B**). This indicated that the difference in pDC numbers seen between NeuN and *galectin-3* KO NeuN mice is specific only to that strain. I also performed the comparison in wildtype C57Bl/6 mice compared to *galectin-3* KO counterparts, and saw a similar outcome to the FVB/N strain, where baseline numbers of lymph node pDCs were comparable to the numbers seen in *galectin-3* KO NeuN mice rather than normal NeuN mice (**Figure 13C**). This indicates that it is the normal NeuN mice that have a deficiency in pDC numbers, not the NeuN *galectin-3* KO mice that have unusually high numbers of these cells.

Plasmacytoid Dendritic Cell Deficiency in NeuN Mice Does Not Extend to Other Tumor Models or Other Immune Cell Compartments

Based on our data in the NeuN mouse model of tumor tolerance, I wanted to learn whether the deficiency in pDC numbers in these mice could be observed in other mouse tumor models. I hypothesized that the loss of pDCs in the NeuN mice could be

Figure 13: *Galectin-3* KO NeuN mice have normal pDC numbers comparable to wildtype and KO mice from background strains while normal NeuN mice have a depletion of this population. Single cell suspensions prepared from lymph nodes of indicated mouse strains were stained for surface markers and gated on pDC markers B220, Ly6C, and CD11c. **A.** Comparison of pDC numbers in lymph nodes of NeuN and NeuN *galectin-3* KO mice shows a pDC deficiency in normal NeuN mice. **B.** Comparison of pDC numbers in lymph nodes of wildtype and *galectin-3* KO FVB/N mice. **C.** Comparison of pDC numbers in lymph nodes of wildtype and *galectin-3* KO C57Bl/6 mice. Only normal NeuN mice show a deficiency in pDCs, and this appears to be rescued upon *galectin-3* KO.

A

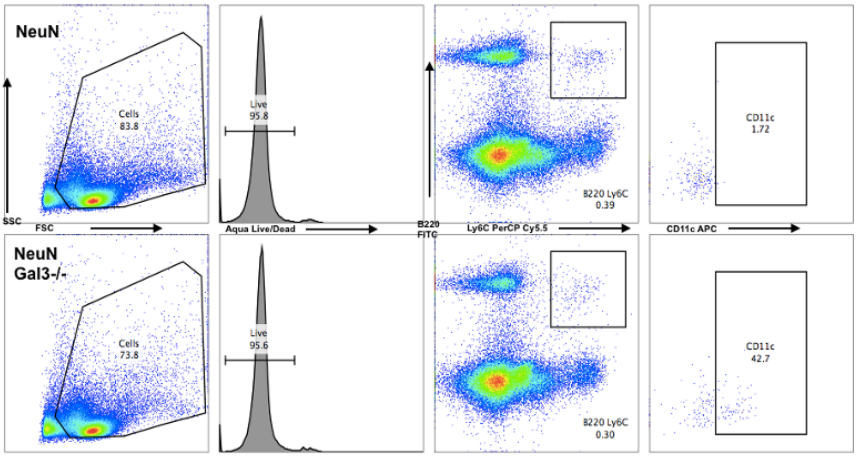
NeuN
Cells
83.8
SSC
FSC
Live
95.8
Aqua Live/Dead
B220
FITC
B220 Ly6C
0.39
Ly6C PerCP Cy5.5
CD11c
1.72
CD11c APC
NeuN
Gal3-/-
Cells
73.8
Live
95.6
B220 Ly6C
0.30
CD11c
42.7

B

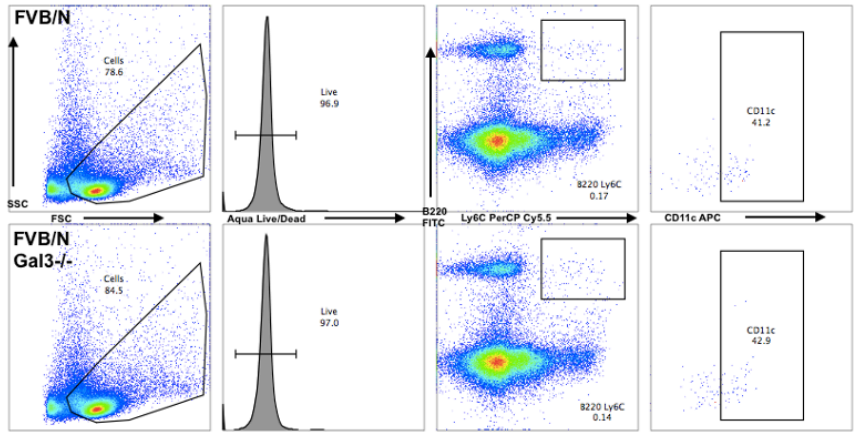
FVB/N
Cells
78.6
SSC
FSC
Live
96.9
Aqua Live/Dead
B220
FITC
B220 Ly6C
0.17
Ly6C PerCP Cy5.5
CD11c
41.2
CD11c APC
FVB/N
Gal3-/-
Cells
84.5
Live
97.0
B220 Ly6C
0.14
CD11c
42.9

C

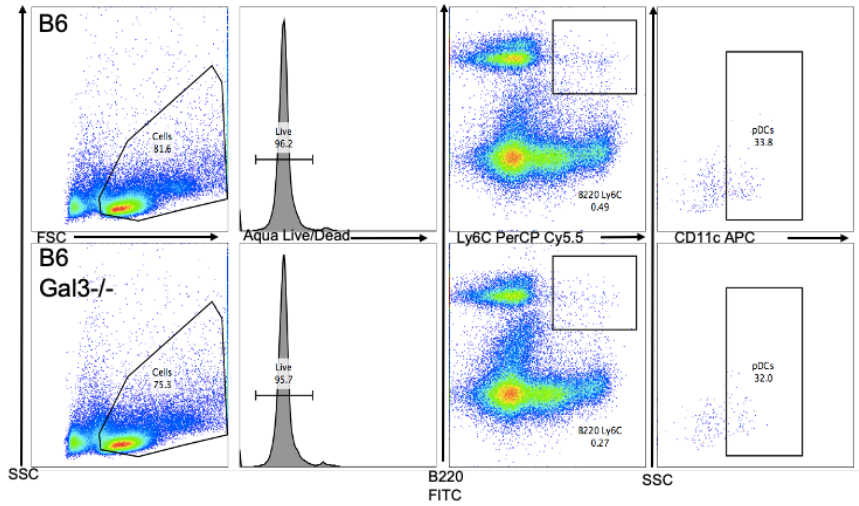
B6
Cells
81.6
Live
96.2
B220 Ly6C
0.49
pDCs
33.8
FSC
Aqua Live/Dead
Ly6C PerCP Cy5.5
CD11c APC
B6
Gal3-/-
Cells
75.3
Live
95.7
B220 Ly6C
0.27
pDCs
32.0
SSC
B220
FITC
SSC

due to the tolerance induced by self-tissue expression of pre-oncogenic Neu in these mice. Other tumor models induce tumor permissiveness through other mechanisms of tolerance induction, but these other mechanisms may cause a similar drop in pDC numbers that I would be able to detect. To this end, I prepared single-cell suspensions from the lymph nodes of KPC and KPC-G mice and performed staining and analysis by flow cytometry to compare the pDC numbers in these mice to those in the NeuN strain. The numbers of pDCs in KPC and KPC-G mice were very similar, and were comparable to the numbers observed in NeuN *galectin-3* KO mice (**Figure 14A**). This outcome indicates that the difference in pDC numbers seen between NeuN and *galectin-3* KO NeuN mice likely occurs only in that strain, and is not due to a mechanism of tolerance held in common between genetically engineered mouse tumor models.

I also investigated other compartments where immune cell subsets reside, to determine whether the decrease in pDC number in the lymph nodes of normal NeuN mice could be due to their migration to a different location. I compared pDCs in the lymph nodes, spleen, and blood of NeuN and NeuN *galectin-3* KO mice, and found that lower pDC numbers are seen in all compartments in the NeuN mice, indicating that the phenomenon is not due to migration of this cell population (**Figure 14B**).

Normal NeuN Mice Have a Deficiency in All CD11c$^+$ Cells

As I investigated the differences in pDC numbers between normal and galectin-3 deficient NeuN mice, I began to consider that this defect may not be restricted to pDC populations. I therefore returned to my previous data that had verified this

Figure 14: pDC deficiency is not shared between the NeuN strain and other mouse strains tolerized to tumor, and is not confined to NeuN lymph nodes. A. Single cell suspensions from lymph nodes of KPC or KPC-G mice were stained for surface markers of pDCs. No difference in pDC numbers was observed between KPC and KPC-G mice. **B.** Single cell suspensions prepared from lymph nodes, spleen, and peripheral blood of normal NeuN or NeuN *galectin-3* KO mice were stained for surface markers of pDCs. pDC deficiency was apparent in all compartments and is not due to differential trafficking of these cells.

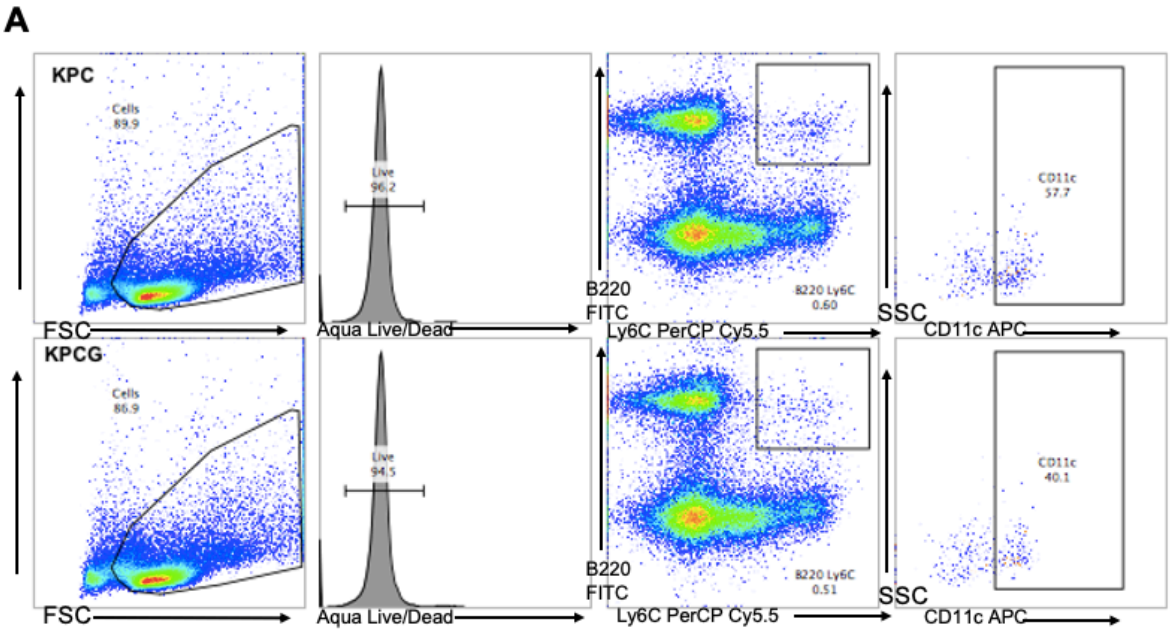
A
KPC
Cells
89.9
FSC
Live
96.2
Aqua Live/Dead
B220
FITC
8220 Ly6C
0.60
Ly6C PerCP Cy5.5
CD11c
57.7
SSC
CD11c APC
KPCG
Cells
86.9
FSC
Live
94.5
Aqua Live/Dead
B220
FITC
8220 Ly6C
0.51
Ly6C PerCP Cy5.5
CD11c
40.1
SSC
CD11c APC

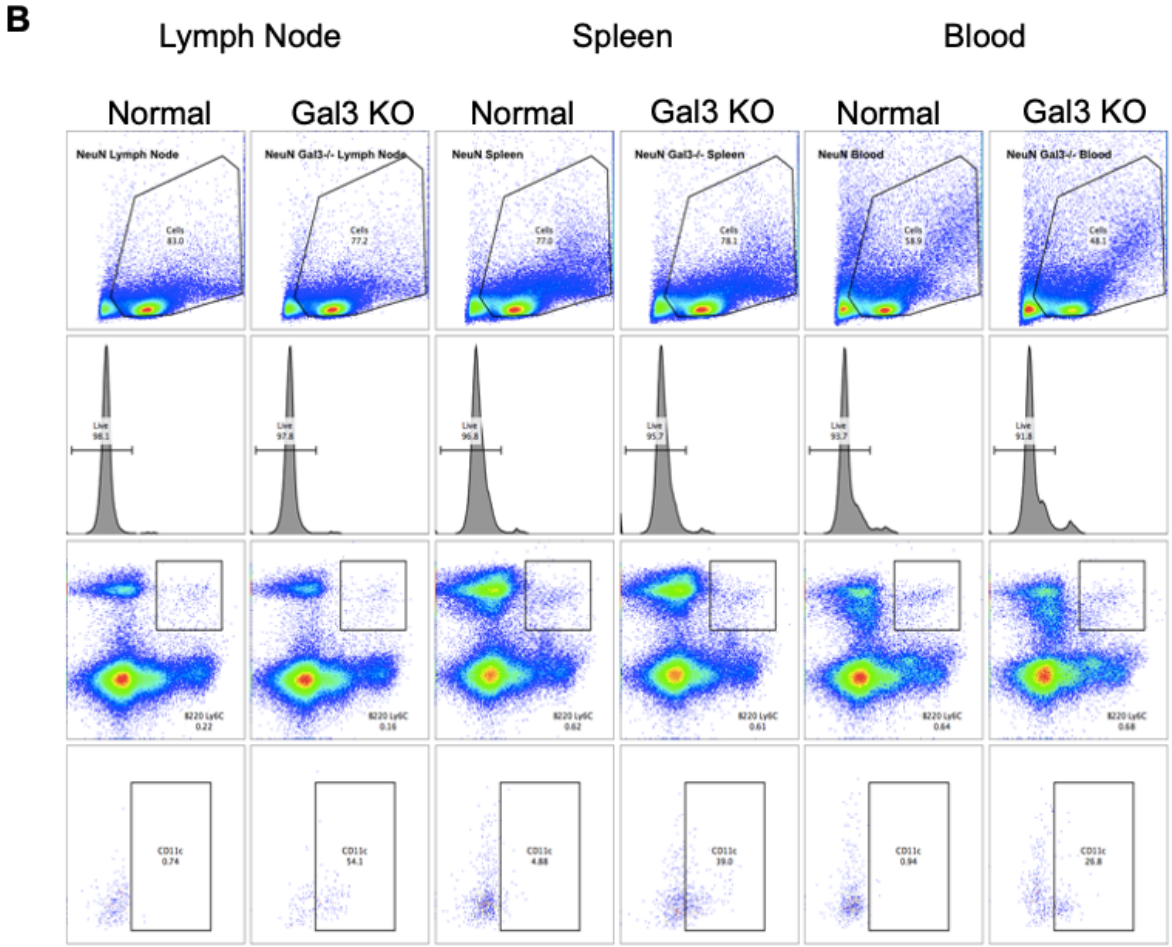
B
Lymph Node
Spleen
Blood
Normal
Gal3 KO
Normal
Gal3 KO
Normal
Gal3 KO
NeuN Lymph Node
NeuN Gal3-/- Lymph Node
NeuN Spleen
NeuN Gal3-/- Spleen
NeuN Blood
NeuN Gal3-/- Blood

deficiency and examined the entire CD11c-expressing cell fraction in these two mouse populations. Indeed, when gating the flow cytometry data broadly by size and granularity, then selecting all live cells and examining the $CD11c^+$ fraction, I found that the deficiency in NeuN mice extended to all $CD11c^+$ cells, rather than being limited to pDCs (**Figure 15**). This finding could have significant implications for the use of the NeuN mouse model in studies of antitumor immunity.

Figure 15: NeuN mice are deficient in all CD11c+ cells, not only pDCs. Single cell suspensions prepared from lymph nodes of normal NeuN mice were stained for surface CD11c. Normal NeuN mice have nearly tenfold fewer CD11c+ cells than their *galectin-3* KO counterparts.

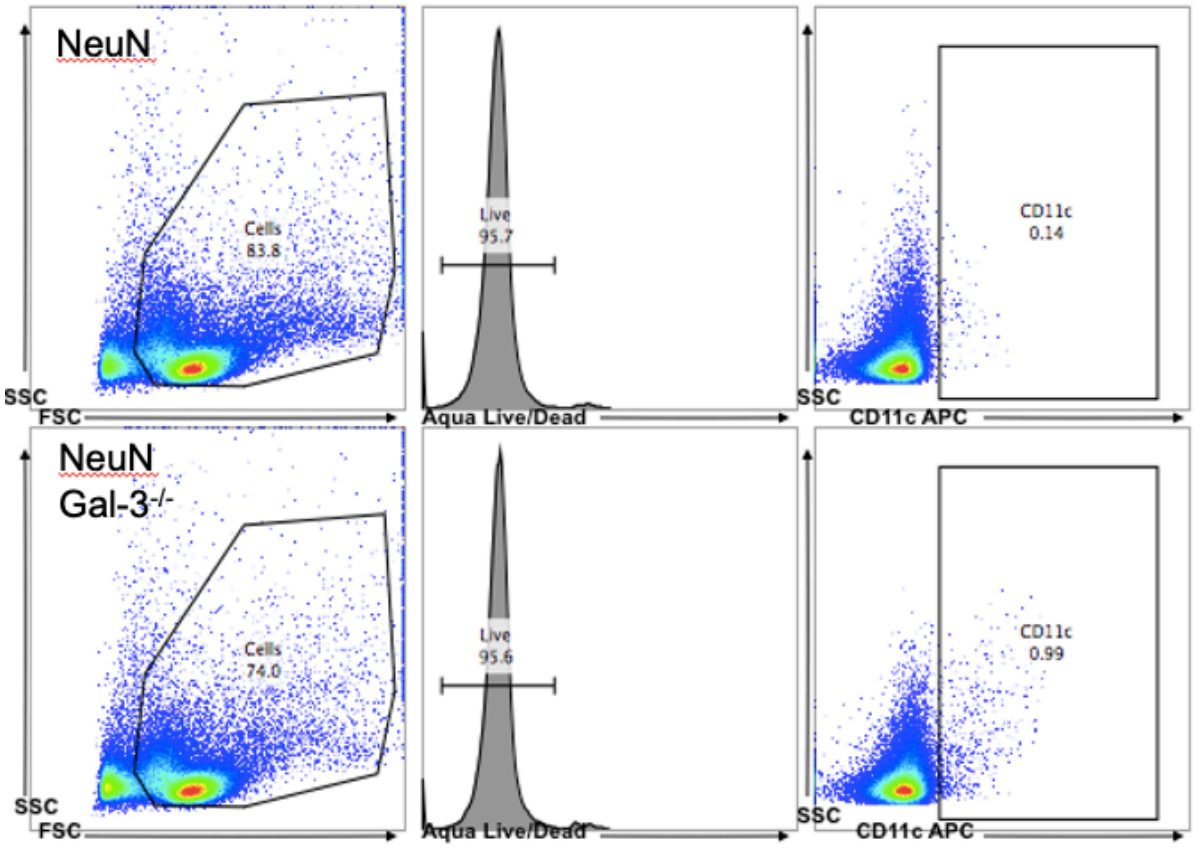

Discussion

Our examination of pDC numbers in the lymph nodes of NeuN mice and their *galectin-3* KO counterparts has revealed that the normal transgenic mice have significantly fewer of these cells. My colleague previously hypothesized that knockout of *galectin-3* led to a more immune-permissive environment where more pDCs could proliferate and present antigen. I disproved this hypothesis by comparing pDC numbers in wildtype and *galectin-3* KO FVB/N and C57Bl/6 mice, all of which have comparable pDC numbers to those seen in *galectin-3* KO NeuN mice. This indicates that there is a deficiency in this cell type in the normal NeuN mice, not an increase in *galectin-3* KO NeuN mice. The cause of this deficiency remains unclear. I hypothesized that it could be caused by mechanisms of tolerance that are shared in common with other genetically-engineered mouse tumor models, and that this strain may not be alone in seeing rescue of pDCs upon galectin-3 abrogation, but in the KPC mouse model there was no detectable deficiency in pDCs, indicating that this phenotype could truly be unique to NeuN mice.

In exploring this deficiency further, I showed that the decrease in pDC numbers in the lymph node is not caused by migration of these cells to the spleen or bloodstream, as all of these compartments demonstrate the deficiency to a similar degree when compared to *galectin-3* KO NeuN mice. By re-analyzing my flow cytometry data, I was able to show that pDCs alone are not the sole deficient population; the entire $CD11c^+$ cell fraction is depleted in these mice. Given the crucial role played by $CD11c^+$ dendritic cells (DCs) in antigen presentation and the induction of effective immune responses, this phenomenon cannot be ignored. Any experiments

performed using NeuN mice should take into account that they lack significant numbers of a very important immune cell subset.

Since NeuN mice are a transgenic strain, I questioned whether the incorporation of the transgene could be disrupting $CD11c^+$ cells in some way. Another group has determined the location of the transgene in NeuN mice, and this does not offer any insights into the depletion of $CD11c^+$ cells (55). Another possibility could be a genetic difference left over from the process of crossing NeuN mice with *galectin-3* KO animals. NeuN *galectin-3* KO mice were made backcrossing *galectin-3* KO mice of the C57Bl/6 background with FVB/N background mice for six generations using a marker-assisted speed congenic approach, and were assessed as having 99.75% identity with the FVB/N background at the final backcross generation (20). This makes the presence of confounding genetic factors unlikely, but cannot be ruled out without performing in-depth genomic analyses of the NeuN mice compared to the NeuN *galectin-3* KO mice.

One very important consideration in this finding is its implications for our previous data on the suppression of $CD8^+$ T cell effector function in NeuN mice. Since CD11c is a marker for many DC subsets, the absence or depletion of all cells carrying this marker in NeuN mice could have profound impacts on $CD8^+$ T cell effector function. It is possible that the suppression of $CD8^+$ T cells in the presence of galectin-3 is not due to a galectin-3 surface binding event, but rather to missing interactions between $CD8^+$ T cells and DCs. Even if surface binding of galectin-3 to $CD8^+$ T cells is involved in their suppression within the TME, a lack of $CD11c^+$ cells could exacerbate this effect.

If congenicity is not a factor in the observed depletion of $CD11c^+$ cells in NeuN mice, abrogation of galectin-3 could truly be rescuing the depletion of an entire cell population. This is yet to be proven, and I have not yet been able to find a compelling answer in the literature for what mechanisms could be at play in such a phenomenon. I do, however, think it possible that there is a yet-undescribed mechanism of peripheral immune tolerance that involves deletion of DC populations. Peripheral tolerance mechanisms that target lymphocytes are well described, but similar mechanisms involving DCs have not been shown. I believe that such mechanisms may exist, and may be used by tumors as a mechanism of immune escape in certain contexts. This subject requires immense further study, and presently remains solely in the realm of conjecture.

CHAPTER 5: Summary

Recent research has cemented galectin-3 as a tumor-promoting force in the tumor microenvironment, as described in Chapter 1. Our lab's past work has shown that mounting an immune response against galectin-3 is correlated with better patient outcomes after receiving a DC-stimulating tumor vaccine, and that healthy $CD8^+$ T cells stimulated *in vitro* have better effector potential in the presence of these patients' serum antibodies than without. Further work showed that galectin-3 is modulating the antitumor capabilities of $CD8^+$ T cells through a mechanism that is not yet fully described (20). My aim has been first, to determine whether galectin-3 acts early enough in the development of PDAC to become a potential target for preventative therapeutics, and second, to develop assays that will allow us to elucidate the mechanisms by which galectin-3 modulates $CD8^+$ T cell function.

In my studies using the KPC mouse model with and without galectin-3, we determined that abrogation of galectin-3 is not impacting PDAC development in a significant manner. While the absence of galectin-3 appeared to have a small effect on the duration of survival for some individuals, further analysis indicated that these differences may be due to sex differences rather than the presence or absence of galectin-3. There is no indication in the current literature that female mice or humans are more susceptible to galectin-3-mediated tumor promotion than males, so the differences we observed are likely not related to the genetic ablation of this protein. In the future, researchers using the KPC mouse model should take these sex-based survival differences into account. Taken together, these data indicate that galectin-3 is not likely to be a top target in the development of PDAC preventative therapeutics.

My other goal was to learn more about the mechanisms through which galectin-3 modulates immune cell function in the context of tumor. Learning more about these mechanisms has required the development of new assays, which I hope will allow study of galectin-3 function and mechanism *in vitro*. I have optimized our lab's *ex vivo* $CD8^+$ T cell re-stimulation assay, and have also developed protocols for the purification of mouse galectin-3 from a mammalian transfection system that will as closely as possible match the function of galectin-3 produced at the tumor site. My ongoing work involves the use of this purified protein to model $CD8^+$ T cell suppression *in vitro*. In this system, we can verify that the mechanism of this suppression is mediated by direct binding of galectin-3 to the T cell surface, and also use galectin-3 mutants to determine the roles its binding domains play in these interactions.

Should our assay fail to show suppression of $CD8^+$ T cells by galectin-3 *in vitro* after activation *in vivo*, we may instead be approaching a new model - a mechanism in which other cell types must be involved to achieve suppression. My colleague previously discovered a discrepancy in pDC numbers between NeuN mice and their *galectin-3* KO counterparts, and I have shown that this discrepancy is actually extended to all $CD11c^+$ DC subsets, and is specific to the NeuN transgenic mouse strain. Since this strain demonstrates heavy suppression of adoptively-transferred antigen-specific $CD8^+$ T cells in the tumor microenvironment, and this effect is mitigated upon knockout of galectin-3, the mechanism could be an indirect one that requires DC involvement. Elucidating this point will require further research as there are no studies in the current literature that describe modulation of DCs by galectin-3 that lead to a suppression of $CD8^+$ T cells.

Study of galectin-3 in the tumor microenvironment is complex, as this protein is extremely multifunctional, placing it at the interface of a multitude of intracellular and extracellular interactions. Elucidation of these mechanisms will require a deep grasp of cellular metabolic changes within the tumor microenvironment, how such changes affect glycosylation and other cellular processes, and how these in turn alter the expression, secretion, and downstream effects of galectin-3. This protein remains a promising target in the quest to program an immune-permissive microenvironment, but its targeting will be incomplete without elucidating all levels of its impact on both tumors and immune cells.

REFERENCES

1. Mellman I, Coukos G, Dranoff G. Cancer immunotherapy comes of age. Nature. 2011;480:480-489.
2. Hanahan D, Weinberg RA. Hallmarks of cancer: The next generation. Cell. 2011;144(5):646–74.
3. Liu FT, Rabinovich GA. Galectins as modulators of tumour progression. Nat Rev Cancer. 2005;5(1):29–41.
4. Khaldoyanidi SK, Glinsky V V, Sikora L, Glinskii AB, Mossine V V, Quinn TP, et al. MDA-MB-435 Human Breast Carcinoma Cell Homo-and Heterotypic Adhesion under Flow Conditions Is Mediated in Part by Thomsen-Friedenreich Antigen-Galectin-3 Interactions. J Biol Chem. 2002;278(6):4127-34.
5. Yang RY, Rabinovich GA, Liu FT. Galectins: Structure, function and therapeutic potential. Exp Rev Mol Med. 2008;10(17).
6. Cummings RD, Liu F, Vasta GR. Chapter 36 Galectins. In: Varki A, Cummings RD, Esko JD, Stanley P, Hart GW, Aebi M, et al., editors. Essentials of Glycobiology Third Edition. 3rd ed. Cold Spring Harbor Laboratory Press; 2017.
7. Rabinovich GA, Toscano MA. Turning “sweet” on immunity: Galectin-glycan interactions in immune tolerance and inflammation. Nat Rev Immunol. 2009;9(5):338–52.
8. Yang R-Y, Hsu DK, Liu F-T, Beutler E. Expression of galectin-3 modulates T-cell growth and apoptosis. Proc Natl Acad Sci. 1996;93(13):6737-42.

9. Fukumori T, Takenaka Y, Oka N, Yoshii T, Hogan V, Inohara H, et al. Endogenous Galectin-3 Determines the Routing of CD95 Apoptotic Signaling Pathways. Cancer Res. 2004;64:3376-79.

10. Liu L, Sakai T, Sano N, Fukui K. Nucling mediates apoptosis by inhibiting expression of galectin-3 through interference with nuclear factor κB signalling. Biochem J. 2004;380(1):31-41.

11. Elad-Sfadia G, Haklai R, Balan E, Kloog Y. Galectin-3 augments K-ras activation and triggers a ras signal that attenuates ERK but not phosphoinositide 3-kinase activity. J Biol Chem. 2004 Aug 13;279(33):34922–30.

12. Lee YJ, Song YK, Song JJ, Rita Siervo-Sassi R, Kim H-RC, Li L, et al. Reconstitution of galectin-3 alters glutathione content and potentiates TRAIL-induced cytotoxicity by dephosphorylation of Akt. Exp Cell Res. 2003;288(1):21-34.

13. Hsu DK, Zuberi RI, Liu FT. Biochemical and biophysical characterization of human recombinant IgE- binding protein, an S-type animal lectin. J Biol Chem. 1992;267(20):14167–74.

14. Ochieng J, Platt D, Tait L, Hogan V, Raz T, Carmi P, et al. Structure-function relationship of a recombinant human galactoside-binding protein. Biochemistry. 1993;32(16):4455–60.

15. Ahmad N, Gabius H-J, André S, Kaltner H, Sabesan S, Roy R, et al. Galectin-3 Precipitates as a Pentamer with Synthetic Multivalent Carbohydrates and Forms Heterogeneous Cross-linked Complexes. 2004;279(12):10841-47.

16. Lin YH, Qiu DC, Chang WH, Yeh YQ, Jeng US, Liu FT, et al. The intrinsically disordered N-terminal domain of galectin-3 dynamically mediates multisite self-association of the protein through fuzzy interactions. J Biol Chem. 2017;292(43):17845–56.

17. Rabinovich GA, Toscano MA, Jackson SS, Vasta GR. Functions of cell surface galectin-glycoprotein lattices. Curr Opin Struct Biol. 2007;17(5):513–20.

18. Wang L-P, Chen S-W, Zhuang S-M, Li H, Song M. Galectin-3 Accelerates the Progression of Oral Tongue Squamous Cell Carcinoma via a Wnt/β-catenin-Dependent Pathway. Pathol Oncol Res. 2013;19(3):461-474.

19. Reticker-Flynn NE, Bhatia SN. Aberrant Glycosylation Promotes Lung Cancer Metastasis through Adhesion to Galectins in the Metastatic Niche. Cancer Discovery. 2014;5(2):168-181.

20. Kouo T, Huang L, Pucsek AB, Cao M, Solt S, Armstrong T, et al. Galectin-3 shapes antitumor immune responses by suppressing CD8 T Cells via LAG-3 and Inhibiting Expansion of Plasmacytoid Dendritic Cells. Cancer Immunol Res. 2015;3(4):412-423.

21. Reiser J, Banerjee A. Review Article Effector, Memory, and Dysfunctional CD8 + T Cell Fates in the Antitumor Immune Response. J Immunol Res. 2016;e8941260.

22. Karanikas V, Colau D, Baurain J-F, Chiari R, Thonnard J, Gutierrez-Roelens I, et al. High Frequency of Cytolytic T Lymphocytes Directed against a Tumor-specific Mutated Antigen Detectable with HLA Tetramers in the Blood of a

Lung Carcinoma Patient with Long Survival. Cancer Res. 2001;61(9):3718-24.

23. Coulie PG, Karanikas V, Colau D, Lurquin C, Landry C, Marchand M, et al. A monoclonal cytolytic T-lymphocyte response observed in a melanoma patient vaccinated with a tumor-specific antigenic peptide encoded by gene MAGE-3. Proc Natl Acad Sci. 2001;98(18):10290-95.
24. Golstein P, Griffiths GM. An early history of T cell-mediated cytotoxicity. Nat Rev Immunol. 2018;18(8):527-535.
25. Pardoll DM. The blockade of immune checkpoints in cancer immunotherapy. Nat Rev Cancer. 2012;12(4):252–64.
26. Guermonprez P, Valladeau J, Zitvogel L, Théry C, Amigorena S. Antigen presentation and T cell stimulation by dendritic cells. Annu Rev Immunol. 2002;20:621–67.
27. Mildner A, Jung S. Development and Function of Dendritic Cell Subsets. Immunity. 2014;40(5):642-656.
28. Fu C, Jiang A. Dendritic Cells and CD8 T Cell Immunity in Tumor Microenvironment. Front Immunol. 2018;9:e3059.
29. Hildner K, Edelson BT, Purtha WE, Diamond M, Matsushita H, Kohyama M, et al. Batf3 deficiency reveals a critical role for CD8α+ dendritic cells in cytotoxic T cell immunity. Science. 2008 Nov 14;322(5904):1097–100.
30. Herber DL, Cao W, Nefedova Y, Novitskiy S V, Nagaraj S, Tyurin VA, et al. Lipid accumulation and dendritic cell dysfunction in cancer. Nat Med. 2010;16(8):880-886.
31. Cao W, Ramakrishnan R, Tuyrin VA, Veglia F, Condamine T, Amoscato A, et

al. Oxidized Lipids Block Antigen Cross-Presentation by Dendritic Cells in Cancer. J Immunol. 2014 Mar 15;192(6):2920–31.

32. Cubillos-Ruiz JR, Silberman PC, Rutkowski MR, Lee A-H, Conejo-Garcia JR, Correspondence LHG, et al. ER Stress Sensor XBP1 Controls Anti-tumor Immunity by Disrupting Dendritic Cell Homeostasis Article ER Stress Sensor XBP1 Controls Anti-tumor Immunity by Disrupting Dendritic Cell Homeostasis. Cell. 2015;161(7):1527-38.

33. Song S, Ji B, Ramachandran V, Wang H, Hafley M, Logsdon C, et al. Overexpressed Galectin-3 in Pancreatic Cancer Induces Cell Proliferation and Invasion by Binding Ras and Activating Ras Signaling. PLoS One. 2012 Aug 10;7(8):e42699.

34. Takenaka Y, Fukumori T, Yoshii T, Oka N, Inohara H, Kim H-RC, et al. Nuclear Export of Phosphorylated Galectin-3 Regulates Its Antiapoptotic Activity in Response to Chemotherapeutic Drugs. Mol Cell Biol. 2004 May 15;24(10):4395–406.

35. Hoyer KK, Pang M, Gui D, Peter Shintaku I, Kuwabara I, Liu F-T, et al. An Anti-Apoptotic Role for Galectin-3 in Diffuse Large B-Cell Lymphomas. Am J Pathol. 2004;164(3)893-902.

36. Nangia-Makker P, Honjo Y, Sarvis R, Akahani S, Hogan V, Pienta KJ, et al. Galectin-3 Induces Endothelial Cell Morphogenesis and Angiogenesis. 2000;156(3):899-909.

37. Demotte N, Stroobant V, Courtoy PJ, Van Der Smissen P, Colau D, Luescher IF, et al. Restoring the Association of the T Cell Receptor with CD8 Reverses

Anergy in Human Tumor-Infiltrating Lymphocytes. Immunity. 2008 Mar 14;28(3):414–24.

38. Fukumori T, Takenaka Y, Yoshii T, Kim H-RC, Hogan V, Inohara H, et al. CD29 and CD7 Mediate Galectin-3-Induced Type II T-Cell Apoptosis. Cancer Res. 2003;63(23)8302-11.

39. Siegel RL, Miller KD, Jemal A. Cancer statistics, 2019. CA Cancer J Clin. 2019 Jan 8;69(1):7–34.

40. Ino Y, Yamazaki-Itoh R, Shimada K, Iwasaki M, Kosuge T, Kanai Y, et al. Immune cell infiltration as an indicator of the immune microenvironment of pancreatic cancer. Br J Cancer. 2013 Mar 5;108(4):914–23.

41. Tuveson DA, Hingorani SR. Ductal pancreatic cancer in humans and mice. In: Cold Spring Harbor Symposia on Quantitative Biology. Cold Spring Harb Symp Quant Biol. 2005;70:65-72.

42. Hingorani SR, Wang L, Multani AS, Combs C, Deramaudt TB, Hruban RH, et al. Trp53 R172H and Kras G12D cooperate to promote chromosomal instability and widely metastatic pancreatic ductal adenocarcinoma in mice. Cancer Cell. 2005;7(5):469-483.

43. Keenan BP, Saenger Y, Kafrouni MI, Leubner A, Lauer P, Maitra A, et al. A Listeria Vaccine and Depletion of T-Regulatory Cells Activate Immunity Against Early Stage Pancreatic Intraepithelial Neoplasms and Prolong Survival of Mice. Gastroenterology. 2014;146:1784-1794.

44. Hruban RH, Maitra A, Goggins M. Update on Pancreatic Intraepithelial Neoplasia. Int J Clin Exp Pathol. 2008;1(4):306-316.

45. Park A-M, Hagiwara S, Hsu DK, Liu F-T, Yoshie O. Galectin-3 Plays an Important Role in Innate Immunity to Gastric Infection by Helicobacter pylori. 2016;84(4):1184-93.

46. Guy CT, Webster MA, Schallert M, Parsonst TJ, Cardifft RD, Muller WJ. Expression of the neu protooncogene in the mammary epithelium of transgenic mice induces metastatic disease. Proc Natl Acad Sci. 1992;89(22)10578-82.

47. Wolpoe ME, Lutz ER, Ercolini AM, Murata S, Ivie SE, Garrett ES, et al. HER-2/neu-Specific Monoclonal Antibodies Collaborate with HER-2/neu-Targeted Granulocyte Macrophage Colony-Stimulating Factor Secreting Whole Cell Vaccination to Augment CD8 + T Cell Effector Function and Tumor-Free Survival in Her-2/ neu -Transgenic Mice . J Immunol. 2003 Aug 15;171(4):2161–9.

48. Weiss VL, Lee TH, Song H, Kouo TS, Black CM, Sgouros G, et al. Trafficking of high avidity HER-2/neu-specific T cells into HER-2/neu-expressing tumors after depletion of effector/memory-like regulatory T cells. PLoS One. 2012;7(2).

49. Xu Y, Chaudhury A, Zhang M, Savoldo B, Metelitsa LS, Rodgers J, et al. Glycolysis determines dichotomous regulation of T cell subsets in hypoxia. J Clin Invest. 2016 Jul 1;126(7):2678–88.

50. Zhang Y, Kurupati R, Liu L, Zhou XY, Zhang G, Hudaihed A, et al. Enhancing CD8+ T Cell Fatty Acid Catabolism within a Metabolically Challenging Tumor Microenvironment Increases the Efficacy of Melanoma Immunotherapy.

Cancer Cell. 2017 Sep 11;32(3):377-391.e9.

51. Wang L, Li S, Yu X, Han Y, Wu Y, Wang S, et al. α2,6-Sialylation promotes immune escape in hepatocarcinoma cells by regulating T cell functions and CD147/MMP signaling. J Physiol Biochem. 2019 Jun 15;75(2):199–207.

52. Demotte N, Bigirimana R, Wieërs G, Stroobant V, Squifflet JL, Carrasco J, et al. A short treatment with galactomannan GM-CT-01 corrects the functions of freshly isolated human tumor-infiltrating lymphocytes. Clin Cancer Res. 2014 Apr 1;20(7):1823–33.

53. Fermino ML, Polli CD, Toledo KA, Liu F-T, Hsu DK, Roque-Barreira MC, et al. LPS-Induced Galectin-3 Oligomerization Results in Enhancement of Neutrophil Activation. PLoS One. 2011 Oct 21;6(10):e26004.

54. Scopes RK. Protein Purification. New York, NY: Springer New York; 1994.

55. Rennhack JP, To B, Swiatnicki M, Dulak C, Ogrodzinski MP, Zhang Y, et al. Integrated analyses of murine breast cancer models reveal critical parallels with human disease. Nat Commun. 2019 Dec 1;10(1):1–12.

CURRICULUM VITAE

The Johns Hopkins University School of Medicine

Alexandra B. Pucsek March 18, 2020

Personal Data

Business Address	733 N Broadway Suite 631 Baltimore, MD 21205
Tel	410-614-1772
Fax	410-614-8216
E-mail	abolm1@jhmi.edu

Education and Training

2009	AB in Biochemical Sciences	Harvard University, Cambridge, MA
2020 (expected)	PhD in Immunology Mentor: Dr. Elizabeth Jaffee	Johns Hopkins University School of Medicine, Baltimore, MD

Professional Experience

2008-2009	Harvard College Research Program Fellowship, Lab of Dr. Max Essex, DVM, PhD	Harvard T.H. Chan School of Public Health, Boston, MA
2009-2011	Research Assistant II, Lab of Dr. Laurie Glimcher, MD	Harvard T.H. Chan School of Public Health, Boston, MA
2012-2013	Research Technologist, Lab of Dr. Christopher Gamper, MD, PhD	Johns Hopkins University School of Medicine

Scholarships and Fellowships

2008-2009 Harvard College Research Program

Publications

Lazarevic V, Chen X, Shim J-H, Hwang E-S, Jang E, **Bolm AB**, Oukka M, Kuchroo VK, Glimcher LH. T-bet represses T_H17 differentiation by preventing Runx1-mediated activation of the gene encoding RORγt. Nat Immunol. 2011;12(1):96-105.

Wang Y, Godec J, Ben-Aissa K, Cui K, Zhao K, **Pucsek AB**, Lee YK, Weaver CT, Yagi R, and Lazarevic V. The Transcription Factors T-bet and Runx Are Required for the Ontogeny of Pathogenic Interferon-g-Producing T Helper 17 Cells. Immunity. 2014;40:355–366.

Kouo T, Huang L, **Pucsek AB**, Cao M, Solt S, Armstrong T, and Jaffee E. Galectin-3 Shapes Antitumor Immune Responses by Suppressing $CD8^+$ T Cells via LAG-3 and Inhibiting Expansion of Plasmacytoid Dendritic Cells. Cancer Immunol Res. 2015; 3(4):412-423.

Ladle BH, Li K, Phillips MJ, **Pucsek AB**, Haile A, Powell JD, Jaffee EM, Hildeman

DA, and Gamper CJ. De novo DNA methylation by DNA methyltransferase 3a controls early effector $CD8^+$ T-cell fate decisions following activation. Proc Natl Acad Sci. 2016;113(38):10631-10636.

Posters and Abstracts

Pucsek AB, Kouo T, Armstrong TD, Jaffee EM. Immune cell modulation by galectin-3 in the PDA tumor microenvironment. Graduate Program in Immunology Annual Retreat 2015. Baltimore, MD. Poster Presentation.

Pucsek AB, Armstrong TD, Jaffee EM. Plasmacytoid dendritic cell modulation by galectin-3 in tumor-tolerant settings. Graduate Program in Immunology Annual Retreat 2016. Baltimore, MD. Poster Presentation.

Pucsek AB, Armstrong TD, Jaffee EM. The influence of galectin-3 binding properties on its tumor-promoting activity. Graduate Program in Immunology Annual Retreat 2018. Baltimore, MD. Oral Presentation.

Pucsek AB, Armstrong TD, Jaffee EM. Determining the influence of galectin-3 binding properties on its suppression of tumor antigen-specific $CD8^+$ T cells. American Association of Cancer Researchers Annual Meeting 2019. Abstract 581. Atlanta, GA. Poster Presentation.

Educational Activities

2017-2018	Teaching Assistant for Graduate Immunology Course

Recognition

2016	First Place, Johns Hopkins School of Medicine Three-Minute Thesis Competition
2016	People's Choice, Johns Hopkins School of Medicine Three-Minute Thesis Competition
2016	Third Place, Maryland State Three-Minute Thesis Competition